Supporting Information

Selectivity of C−H *vs.* C−F Bond Oxygenation in Homo- and Heterometallic Fe_4, Fe_3Mn, and Mn_4 Clusters

Dr. Graham de Ruiter,[a] Kurtis M. Carsch,[a] Michael K. Takase, and Prof. Theodor Agapie*[a]

[a]*Department of Chemistry and Chemical Engineering. California Institute of Technology; Pasadena, California 91125, United States.*

Table of Contents.

General Considerations.

All reactions were performed at room temperature in an N_2-filled M. Braun Glovebox or by using standard Schlenk techniques unless otherwise specified. Glassware was oven dried at 140 °C for at least 2h prior to use, and allowed to cool under vacuum. All reagents were used as received unless otherwise stated. Iodosobenzene (PhIO), 2-(tertbutylsulfonyl)iodosobenzene (^{s}PhIO), 3-(2-fluorophenyl)-*1H*-pyrazole (HFArPzH), 2-(1H-pyrazol-3-yl)phenolate (NaOArPzH), 2-(1H-pyrazol-3-yl)-3-fluorophenolate (NaOFArPzH), $LFe_3(OAc)(OTf)_2$, and $LMn_3(OAc)(OTf)_2$ were synthesized according to published procedures.[S1-7] *Caution! Iodosobenzene is potentially explosive and should be used only in small quantities.* 2-fluoroacetophenone, Na(N(SiMe3)2), and AgOTf, were purchased from Sigma Aldrich, Oakwood Chemicals and Strem Chemicals. All pyrazoles were sublimed before use. Anhydrous tetrahydrofuran (THF) was purchased from Aldrich in 18 L Pure-Pac^{TM} containers. Anhydrous CH_2Cl_2, diethyl ether, hexane and THF were purified by sparging with nitrogen for 15 minutes and then passing under nitrogen pressure through a column of activated A2 alumina. Anhydrous 1,2-dimethoxyethane (DME) was dried over sodium/benzophenone and vacuum-transferred onto molecular sieves. The ^{1}H and $^{13}C\{^{1}H\}$ NMR spectra were recorded at 400.13, and 100.62 MHz on a Bruker AscendTM 400 MHz spectrometer equipped with prodigy cryoprobe, or at 300.13, 282.36 (^{19}F), and 75.47 MHz, on a Varian 300 MHz spectrometer. All chemical shifts (δ) are reported in ppm, and coupling constants (*J*) are in Hz. The ^{1}H and $^{13}C\{^{1}H\}$ NMR spectra were referenced using residual solvent peaks in the deuterated solvent. The ^{19}F chemical shifts are reported relative to the internal lock signal. Deuterated solvents (CD_2Cl_2 and CD_3CN) were purchased from Cambridge Isotope Laboratories, dried over calcium hydride, degassed by three freeze-pump-thaw cycles and vacuum-transferred prior to use. The UV-vis spectra were recorded on a Varian Cary Bio 50 spectrophotometer. Fast atom bombardment-mass spectrometry (FAB-MS) analysis was performed with a JEOL JMS-600H high resolution mass spectrometer. Elemental analyses were performed at Caltech.

Physical Methods.

Electrochemical measurements. CVs were recorded with a Pine Instrument Company AFCBP1 bipotentiostat using the AfterMath software package. All measurements were performed in a three-electrode cell configuration that consisted of 1) a glassy-carbon (ø = 3.0 mm) working electrode, 2) a Pt wire as counter electrode, and 3) an Ag wire as reference electrode. All electrochemical measurements were performed at RT in an M. Braun N_2-filled glovebox. Dry dichloromethane containing 0.1 M

$^{n}Bu_4NPF_6$ was used as the electrolyte solution. The ferrocene/ferrocenium (Fc/Fc^+) redox couple was used as an internal standard for all measurements.

X-ray crystallography. For compounds **1** and **2**, low-temperature (100 K) diffraction data (ϕ-and ω-scans) were collected on a Bruker AXS D8 VENTURE KAPPA diffractometer coupled to a PHOTON 100 CMOS detectors with Mo Kα radiation (λ = 0.71073 Å) or with Cu Kα (λ = 1.54178 Å). For compound **3**, low-temperature (100 K) diffraction data (ϕ-and ω-scans) were collected on a Bruker AXS KAPPA APEX II diffractometer coupled to an APEX II CCD detector with graphite monochromated Mo Kα radiation (λ = 0.71073 Å). All diffractometer manipulations, including data collection, integration, and scaling were carried out using the Bruker APEXII software.[S8] Absorption corrections were applied using SADABS.[S9] Structures were solved by direct methods using SHELXS[S10] and refined against F^2 on all data by full-matrix least squares with SHELXL-2014[S11] using established refinement techniques.[S12] All non-hydrogen atoms were refined anisotropically. All hydrogen atoms were included into the model at geometrically calculated positions and refined using a riding model. The isotropic displacement parameters of all hydrogen atoms were fixed to 1.2 times the *U* value of the atoms they are linked to (1.5 times for methyl groups). All disordered atoms were refined with the help of similarity restraints on the 1,2- and 1,3-distances and displacement parameters as well as enhanced rigid bond restraints for anisotropic displacement parameters. Due to the size of compounds (**1**–**3**), most crystals included solvent accessible voids, which tended to contain disordered solvent. In most cases, this disorder could be modeled satisfactorily Furthermore, the long-range order of these crystals and amount of high angle data was in some cases not ideal, due to desolvation of the crystals and/or solvent disorder. These disordered solvent molecules were largely responsible for the alerts generated by the checkCIF protocol.

Synthetic Procedures

Sodium 3-(2-fluorophenyl)pyrazolate (NaHFArPz). In the glovebox, to a solution of 3-(2-fluorophenyl)-1H-pyrazole (3.94 g.; 24.0 mmol) in THF (20 mL) was added a solution of sodium bis(trimethylsilyl)amide (5.35 g; 29.0 mmol) in THF (5 mL). The color darkens to light yellow and the homogenous solution was stirred for 2 h. The solvent was removed under reduced pressure to yield a yellow oil. Addition of hexane (50.0 mL), and stirring for 16 h, resulted in the formation of a white precipitate, which was collected on a medium porosity frit. The solid was washed with hexane (3 × 20.0 mL) and dried under reduced pressure to yield of sodium 3-(2-fluorophenyl)pyrazolate (2.0 g; 50 %) as an off-white powder. ^{1}H NMR (400 MHz, CD_3CN) δ 7.94 (td, *J* = 7.8, 1.7 Hz, 1H; *m*-ArH), 7.61 (d, *J* = 1.6 Hz, 1H; CHC*H*NH), 7.18 – 7.05 (m, 3H; *o*-Ar*H*, *m*-Ar*H*, and *p*-Ar*H*), 6.54 (dd, *J* = 3.9, 1.6 Hz, 1H; C*H*CHNH). ^{13}C NMR (101 MHz, CD_3CN) δ 159.93 (d, *J* = 243.8 Hz; *o*-Ar*C*F), 146.12 (d, *J* = 3.8 Hz; NCHCH*C*), 140.89 (d, *J* = 1.7 Hz; N*C*HCHC), 129.29 (d, *J* = 5.3 Hz; *p*-Ar*C*), 127.04 (d, *J* = 8.4 Hz; *o*-Ar*C*), 125.85 (d, *J* = 12.5 Hz; *i*-Ar*C*), 125.05 (d, *J* = 3.1 Hz; *m*-Ar*C*), 116.56 (d, *J* = 23.3 Hz; *m*-Ar*C*), 103.94 (d, *J* = 6.7 Hz; NCH*C*HC). ^{19}F NMR (376 MHz, CD_3CN) δ -118.27 (*o*-Ar*F*).

$[LFe_3(HFArPz)_3OFe][OTf]_2$ (1). In the glovebox, a suspension of $LFe_3(OAc)(OTf)_2$ (4090 mg, 3.0 mmol) in THF (100 mL) was frozen in the cold well. To the thawing suspension was added a thawing solution of NaHFArPz (1820 mg, 10.0 mmol) in THF (6 mL). The color changed immediately to orange and the suspension became homogeneous during the course of 1 hour. The solution was stirred for a total of 2 hours, and a fine suspension was formed. Here after iodosobenzene (PhIO, 671 mg, 3.0 mmol) was added as a solid, and the mixture changed to orange brown immediately and became homogenous after 0.5 h. The solution was stirred for 1 h. and a brown precipitate formed. To the suspension was added $Fe(OTf)_2$ (1562 mg, 4.5 mmol) as a solid. The suspension was stirred for 24 h and subsequently filtered over a bed of Celite (0.5 cm) on a medium porosity glass frit. The remaining brown solid was dissolved in dichloromethane, filtered, and the solvent removed under reduced pressure to yield a brown solid (1763 mg). The solid was crystallized from acetonitrile/diethyl ether to yield $[LFe_3(PhPz)_3OFe][OTf]_2$ as a brown crystals. Yield 1362 mg (24%). X-ray quality crystals were obtained by diffusing diethyl ether into a concentrated solution of **1** in acetonitrile. ^{1}H NMR (300 MHz, CD_2Cl_2) δ 117.5 (br), 70.5 (s), 67.67 (s), 54.3 (br), 49.2 (s), 44.1 (s), 43.6 (s), 17.04 (s), 15.8 (s), 14.6 (s), 12.9 (s), 11.0 (s), -3.56 (s), -7.8 (s). ^{19}F NMR (282 MHz, CD_2Cl_2) δ -78.1 (s). UV-Vis (CH_2Cl_2) [ε (M^{-1} cm^{-1})]: 243 nm (2.43×10^5), 426 nm (2.01×10^4). Anal. calcd. (%) for $C_{86}H_{57}F_9Fe_4N_{12}O_{10}S_2$: C 55.03, H 3.06, N 8.96; found: C 54.59, H 3.10, N 8.68.

[$LFe_3(HFArPz)_3OMn$][$OTf]_2$ (2). In the glovebox, a suspension of $LFe_3(OAc)(OTf)_2$ (4210 mg, 3.0 mmol) in THF (100 mL) was frozen in the cold well. To the thawing suspension was added a thawing solution of NaHFArPz (1902 mg, 10.0 mmol) in THF (6 mL). The color changed immediately to orange and the suspension became homogeneous during the course of 1 hour. The solution was stirred for a total of 2 hours. Here after iodosobenzene (PhIO, 664 mg, 3.0 mmol) was added as a solid, and the mixture changed to orange brown immediately and became homogenous after 0.5 h. The solution was stirred for 1 h. and a brown precipitate formed. To the suspension was added $Mn(OTf)_2$•2MeCN (1926 mg, 4.5 mmol) as a solid. The suspension was stirred for 24 h and the solvent removed under reduced pressure. To the remaining brown solid was added DME (40 mL), and the resulting suspension was stirred for 16 h, and subsequently filtered over a bed of Celite (0.5 cm) on a medium porosity glass frit. The remaining brown solid was dissolved in dichloromethane, filtered, and the solvent removed under reduced pressure to yield a brown solid (2162 mg). The solid was crystallized from acetonitrile/diethyl ether to yield [$LFe_3(PhPz)_3OMn$][$OTf]_2$ as a brown crystals. Yield 1736 mg (31%). X-ray quality crystals were obtained by diffusing diethyl ether into a concentrated solution of **2** in acetonitrile. ^{1}H NMR (300 MHz, CD_2Cl_2) δ 119.0 (br), 78.7 (br), 71.6 (s), 69.7 (s), 53.8 (s), 51.4 (s), 45.4 (s), 15.3 (s), 13.4 (s), -1.9 (s). ^{19}F NMR (282 MHz, CD_2Cl_2) δ -78.1 (s). UV-Vis (CH_2Cl_2) [ε (M^{-1} cm^{-1})]: 244 nm (1.99×10^5), 438 nm (1.48×10^4). Anal. calcd. (%) for $C_{86}H_{57}F_9Fe_3MnN_{12}O_{10}S_2$: C 55.06, H 3.06, N 8.96; found: C 55.03, H 3.34, N 8.28.

[$LMn_3(HFArPz)_3OMn$][$OTf]_2$ (3). In the glovebox, a suspension of $LMn_3(OAc)(OTf)_2$ (2016 mg, 1.5 mmol) in DCM (30 mL) was frozen in the cold well. To the thawing suspension was added a thawing solution of NaHFArPz (1009 mg, 5.5 mmol) in THF (6 mL). The color changed immediately to pink and later to violet, during which the suspension became homogeneous. After stirring for 2 hours, a violet suspension was formed to which was added (PhIO, 336 mg, 1.5 mmol) as a solid. Upon addition of PhIO the color first changed to pink and after stirring for 16 hours a brown suspension was obtained. The solvent was removed under reduced pressure, to yield a brown solid. The solid was suspended in DME and stirred for 16 hours. The solid was collected on a bed of Celite (0.5 cm) on a medium porosity glass frit, and washed with DME until the filtrate was nearly colorless. The remaining solid was dissolved in a minimal of DCM and collected. The solvent was removed under reduced pressure to a brown violet solid (1060 mg). The violet solid was suspended in THF and $Mn(OTf)_2$•2MeCN (1010 mg, 2.2 mmol) was added as a solid. The suspension was stirred for 24 h and the solvent removed under reduced pressure. To the remaining brown/violet solid was added DME (40 mL), and the resulting suspension was stirred for 16 h, and subsequently filtered over a bed of Celite (0.5 cm) on a medium porosity glass frit. The remaining brown solid was dissolved in dichloromethane, filtered, and the solvent removed under reduced

pressure to yield a brown solid (1300 mg). The solid was crystallized from acetonitrile/diethyl ether to yield $[LMn_3(PhPz)_3OMn][OTf]_2$ as a brown/violet crystals. Yield 960 mg (34%). X-ray quality crystals were obtained by diffusing diethyl ether into a concentrated solution of **2** in acetonitrile. ^{1}H NMR (300 MHz, CD_2Cl_2) δ 57.2 (br), 50.3 (s), 34.4 (s), 30.6 (s), 13.8 (s), 10.63 (s), -11.59 (s), -19.43 (s), -32.5 (br). ^{19}F NMR (282 MHz CD_2Cl_2) δ -77.47. UV-Vis (CH_2Cl_2) [ε (M^{-1} cm^{-1})]: 248 nm (2.56×10^5), 500 nm (3.37×10^3). Anal. calcd. (%) for $C_{86}H_{57}F_9Mn_4N_{12}O_{10}S_2$: C 55.14, H 3.07, N 8.97; found: C 55.24, H 3.17, N 9.14.

$[LFe_3(HFArPz)_2(OArPz)OFe][OTf]_2$ (4). In the glovebox, to a solution of $[LFe_3(HFArPz)_3OFe][OTf]_2$ (100.9 mg; 0.054 mmol) in CH_2Cl_2 (5.0 mL) was added a suspension 2-(1*H*-pyrazol-3-yl)-3-phenolate (NaOArPzH; 14.8 mg; 0.082 mmol) in CH_2Cl_2 (1.0 mL). The solution was stirred for ca. 48 h., during which the color changed from brown to red/brown. The solution was filtered over a bed of Celite (0.5 cm) in a glass pipette and the solvent was removed under reduced pressure to yield a red/brown powder (98.2 mg). The crude solid was dissolved in CH_2Cl_2 (5.0 mL) and 400 μL stock solution of 0.12 M AgOTf in MeCN was added (AgOTf stock: 61.6 mg in 2 mL). The solution turned green immediately and was stirred for 2 hours, before the solution was filtered over a bed of Celite (0.5 cm) in a glass pipette to remove metallic Ag. The solvent was removed under reduced pressure to yield of $[LFe_3(HFArPz)_2(OArPz)OFe][OTf]_2$ (**4**) as a green powder. Yield 95.4 mg (94%). If needed compound **4** can be crystallized by vapor diffusion of diethyl ether into a concentrated solution of **4** in MeCN (*ca.* 200 mg mL^{-1}). ^{1}H NMR (300 MHz, CD_2Cl_2) δ 149.1 (br), 140.6 (br), 128.3 (br), 112.9 (br), 103.9 (br), 88.4 (s), 84.7 (br), 82. 5 (s), 81.8 (s), 79.9 (s), 75.4 (s), 69.2 (s), 66.3 (s), 65.1 (s), 62.9 (s), 59.3 (s), 54.7 (s), 47.3 (s), 38.1 (s), 36.0 (s), 31.9 (s), 28.2 (s), -4.5 (br), -7.7 (br), -11.1 (s), -18.6 (br), -21.1 (s). ^{19}F NMR (282 MHz, CD_2Cl_2) δ -77.1, -78.2, -78.9. UV-Vis (CH_2Cl_2) [ε (M^{-1} cm^{-1})]: 243 nm (1.07×10^5), 355 nm (1.17×10^4), 443 nm (8.40×10^3), 596 nm (4.44×10^3). Anal. calcd. (%) for $C_{86}H_{57}F_8Fe_4N_{12}O_{11}S_2$: C 55.12, H 3.07, N 8.97; found: C 54.76, H 3.20, N 8.68.

$[LFe_3(HFArPz)_2(OFArPz)OFe][OTf]_2$ (5). In the glovebox, to a solution of $[LFe_3(HFArPz)_3OFe][OTf]_2$ (91.6 mg; 0.049 mmol) in CH_2Cl_2 (5.0 mL) was added a suspension 2-(1*H*-pyrazol-3-yl)-3-fluorophenolate (NaOFArPzH; 16.7 mg; 0.084 mmol) in CH_2Cl_2 (1.0 mL). The solution was stirred for ca. 48 h., during which the color changed from brown to red/brown. The solution was filtered over a bed of Celite (0.5 cm) in a glass pipette and the solvent was removed under reduced pressure to yield a red/brown powder (73.2 mg). The crude solid was dissolved in CH_2Cl_2 (5.0 mL) and 350 μL stock solution of 0.12 M AgOTf in MeCN was added (AgOTf stock: 61.2 mg in 2 mL). The solution turned green brown immediately and was stirred for 2 hours, before the solution was filtered over a bed of Celite

(0.5 cm) in a glass pipette to remove metallic Ag. The solvent was removed under reduced pressure to yield of $[LFe_3(HFArPz)_2(OFArPz)OFe][OTf]_2$ (**5**) as a green/brown powder. Yield 73.4 mg (81%). If needed compound **5** can be crystallized by vapor diffusion of diethyl ether into a concentrated solution of **5** in MeCN (*ca.* 200 mg mL^{-1}). ^1H NMR (300 MHz, CD_2Cl_2) δ 147.4 (br), 144.0 (br), 129.2 (br), 110.9 (br), 105.8 (br), 88.8 (s), 87.3 (br), 83.3 (s), 82.5 (s), 80.6 (s), 79.9 (s), 77.4 (s), 68.7 (s), 66.4 (s), 65.2 (s), 64.3 (s), 60.1 (s), 55.8 (s), 47.2 (s), 40.1 (s), 36.5 (s), 33.1 (s), 28.4 (s), -2.4 (br), -4.5 (br), -8.3 (br), -17.1 (br), -20.5 (s). ^{19}F NMR (282 MHz, CD_2Cl_2) δ -50.63, -76.94, -78.17. UV-Vis (CH_2Cl_2) [ε (M^{-1} cm^{-1})]: 239 nm (1.06×10^5), 347 nm (1.14×10^4), 443 nm (8.23×10^3), 604 nm (4.16×10^3). Anal. calcd. (%) for $C_{86}H_{56}F_9Fe_4N_{12}O_{11}S_2$: C 54.60, H 2.98, N 8.88; found: C 54.61, H 3.25, N 9.07.

$[LFe_3(HFArPz)_2(OArPz)OMn][OTf]_2$ (6). In the glovebox, to a solution of $[LFe_3(HFArPz)_3OMn][OTf]_2$ (94.6 mg; 0.051 mmol) in CH_2Cl_2 (5.0 mL) was added a suspension 2-(1*H*-pyrazol-3-yl)-3-phenolate (NaOArPzH; 14.2 mg; 0.078 mmol) in CH_2Cl_2 (1.0 mL). The solution was stirred for ca. 48 h., and no clear color change was observed. The solution was filtered over a bed of Celite (0.5 cm) in a glass pipette and the solvent was removed under reduced pressure to yield a brown powder (83.6 mg). The crude solid was dissolved in CH_2Cl_2 (5.0 mL) and 400 μL stock solution of 0.12 M AgOTf in MeCN was added (AgOTf stock: 61.6 mg in 2 mL). The solution turned dark brown immediately and was stirred for 2 hours, before the solution was filtered over a bed of Celite (0.5 cm) in a glass pipette to remove metallic Ag. The solvent was removed under reduced pressure to yield of $[LFe_3(HFArPz)_2(OArPz)OMn][OTf]_2$ (**6**) as a brown powder. Yield 80.3 mg (84%). If needed compound **6** can be crystallized by vapor diffusion of diethyl ether into a concentrated solution of **6** in MeCN (*ca.* 200 mg mL^{-1}). ^1H NMR (300 MHz, CD_2Cl_2) δ 164.5 (br), 158.0 (br), 124.3 (br), 114.5 (br), 107.1 (br), 94.9 (s), 92.5 (s), 88.2 (s), 87.3 (s), 82.5 (s), 75.0 (s), 74.0 (s), 73.3 (s), 70.2 (s), 68.8 (s), 67.9 (s), 62.0 (s), 60.8 (s), 55.7 (s), -7.1 (br). ^{19}F NMR (282 MHz, CD_2Cl_2) δ -77.9, -81.2. UV-Vis (CH_2Cl_2) [ε (M^{-1} cm^{-1})]: 242 nm (2.50×10^5), 450 nm (1.59×10^4). Anal. calcd. (%) for $C_{86}H_{57}F_8Fe_3MnN_{12}O_{11}S_2$: C 55.15, H 3.07, N 8.97; found: C 53.97, H 3.13, N 8.86.

$[LFe_3(HFArPz)_2(OFArPz)OMn][OTf]_2$ (7). In the glovebox, to a solution of $[LFe_3(HFArPz)_3OMn][OTf]_2$ (89.9 mg; 0.048 mmol) in CH_2Cl_2 (5.0 mL) was added a suspension 2-(1*H*-pyrazol-3-yl)-3-fluorophenolate (NaOFArPzH; 16.9 mg; 0.085 mmol) in CH_2Cl_2 (1.0 mL). The solution was stirred for ca. 48 h., during which no apparent color change could be observed. The solution was filtered over a bed of Celite (0.5 cm) in a glass pipette and the solvent was removed under reduced pressure to yield a red/brown powder (86.3 mg). The crude solid was dissolved in CH_2Cl_2 (5.0 mL) and 400 μL stock solution of 0.12 M AgOTf in MeCN was added (AgOTf stock: 61.2 mg in 2 mL). The

solution turned dark brown immediately and was stirred for 2 hours, before the solution was filtered over a bed of Celite (0.5 cm) in a glass pipette to remove metallic Ag. The solvent was removed under reduced pressure to yield of $[LFe_3(HFArPz)_2(OFArPz)OMn][OTf]_2$ (**7**) as a brown powder. Yield 88.6 mg (97%). If needed compound **7** can be crystallized by vapor diffusion of diethyl ether into a concentrated solution of **7** in MeCN (*ca.* 200 mg mL^{-1}). ^1H NMR (300 MHz, CD_2Cl_2) δ 171.7 (br), 162.9 (br), 149.5 (br), 123.7 (br), 119. 3 (br), 97.3 (s), 92.2 (s), 87.7 (s), 85.0 (s), 80.7 (s), 77.2 (s), 73.6 (s), 73.2 (s0, 71.4 (s), 66.7 (s), 62.9 (s), 53.9 (s), -4.9 (br). ^{19}F NMR (282 MHz, CD_2Cl_2) δ -64.6, -77.8, -82.5. UV-Vis (CH_2Cl_2) [ε (M^{-1} cm^{-1})]: 242 nm (1.46×10^5) 450 nm (8.32×10^3) Anal. calcd. (%) for $C_{86}H_{56}F_9Fe_3Mn_{12}O_{11}S_2$: C 54.62, H 2.99, N 8.89; found: C 54.14, H 3.22, N 8.72.

Addition of ^{s}PhIO to $[LFe_3(HFArPz)_3OFe][OTf]_2$ (1). In the glovebox, to a solution of $[LFe_3(HFArPz)_3OFe][OTf]_2$ (56.1 mg; 0.03 mmol) in CH_2Cl_2 (3.0 mL) was added a solution of ^{s}PhIO (21.1 mg; 0.06 mmol) in CH_2Cl_2 (1.0 mL). Upon addition, the color changed immediately to green/black and the solution was stirred for 30 min, where after a 10 μL aliquot was taken, from which the ESI-MS spectrum was recorded. From the remaining solution, the solvent was removed under reduced pressure to yield a green/black solid. The ^1H NMR spectrum of the remaining solid was recorded and showed complex **4** as the major component of the reaction mixture (Figure S8). This procedure was repeated three times to get accurate values on the degree of $C(sp^2)$–H vs. $C(sp^2)$–F activation ^1H NMR and ESI-MS.

Addition of ^{s}PhIO to $[LFe_3(HFArPz)_3OMn][OTf]_2$ (2). In the glovebox, to a solution of $[LFe_3(HFArPz)_3OMn][OTf]_2$ (54.1 mg; 0.03 mmol) in CH_2Cl_2 (3.0 mL) was added a solution of ^{s}PhIO (19.6 mg; 0.06 mmol) in CH_2Cl_2 (1.0 mL). Upon addition, the color darkened to dark brown and the solution was stirred for 45 min, where after a 5 μL aliquot was taken, from which the ESI-MS spectrum was recorded. From the remaining solution, the solvent was removed under reduced pressure to yield a green/black solid. The ^1H NMR spectrum of the remaining solid was recorded and showed complex **7** as the major component of the reaction mixture (Figure S12). This procedure was repeated three times to get accurate values on the degree of $C(sp^2)$–H vs. $C(sp^2)$–F activation by ^1H NMR and ESI-MS.

Addition of ^{s}PhIO to $[LMn_3(HFArPz)_3OMn][OTf]_2$ (3). In the glovebox, to a solution of $[LMn_3(HFArPz)_3OMn][OTf]_2$ (34.1 mg; 0.018 mmol) in CH_2Cl_2 (3.0 mL) was added a solution of ^{s}PhIO (19.6 mg; 0.047 mmol) in CH_2Cl_2 (1.0 mL). Upon addition, the color darkened to dark brown and the solution was stirred for 60 min, where after a 5 μL aliquot was taken, from which the ESI-MS spectrum was recorded. From the remaining solution, the solvent was removed under reduced pressure to yield a

green/black solid. The ^{1}H NMR spectrum of the remaining solid was recorded, but due to paramagnetic broadening by manganese, no useful comparison could be made (Figure S14).

Calibration Curve of Complexes 4 and 5. To get an idea about the extent of C(sp^2)–H vs. C(sp^2)–F bond oxygenation with complex **1**, a calibration curve was constructed according to the following procedure. In the glovebox, separate equimolar stock solutions of $[LFe_3(HFArPz)_2(OArPz)OFe][OTf]_2$ (26.9 mg, 0.014 mmol), and $[LFe_3(HFArPz)_2(OFArPz)OFe][OTf]_2$ (27.1 mg, 0.014 mmol) in CD_2Cl_2 (3.0 mL) were prepared. The equimolar solutions (4.76 mM) of complexes **4** and **5** were subsequently mixed in varying ratios ranging from 5:1 → 1:5, by combining 100 μL stock solutions of each complex to a total volume of 0.6 mL. For example, a 5:1 ratio of complex **4** to **5** was obtained by combining a 500 μL stock solution of **4** with a 100 μL stock solution of **5**. The ^{1}H NMR of all stock solutions were recorded, and their ratio determined by integrating the resonances at 31.8 ppm and 33.0 ppm belonging complexes **4** and **5** respectively. The calibration curve based on NMR spectroscopy was constructed by plotting the experimentally observed ratio (NMR) vs. the ratio in which the complexes were mixed. The calibration curve based on mass spectrometry data, was constructed by taken 5 μL aliquots of the NMR samples (diluted in 1.5 mL MeCN), and plotting the ratios of the ESI-MS peak at m/z = 787.59 (**4**) and at *m/z* = 796.59 (**5**), vs. the ratio in which the complexes were mixed. The NMR and ESI-MS data and the corresponding calibration curves are shown in Figures S18-S20.

Calibration Curve of Complexes 6 and 7. To get an idea about the extent of C(sp^2)–H vs. C(sp^2)–F bond oxygenation with complex **2**, a calibration curve was constructed according to the following procedure. In the glovebox, separate equimolar stock solutions of $[LFe_3(HFArPz)_2(OArPz)OMn][OTf]_2$ (38.2 mg, 0.02 mmol), and $[LFe_3(HFArPz)_2(OFArPz)OFe][OTf]_2$ (38.9 mg, 0.02 mmol) in CD_2Cl_2 (3.0 mL) were prepared. The equimolar solutions (6.79 mM) of complexes **6** and **7** were subsequently mixed in varying ratios ranging from 5:1 → 1:5, by combining 100 μL stock solutions of each complex to a total volume of 0.6 mL. For example, a 5:1 ratio of complex **4** to **5** was obtained by combining a 500 μL stock solution of **4** with a 100 μL stock solution of **5**. The ^{1}H NMR of all stock solutions were recorded, and their ratio determined by integrating the resonances at 60.3 ppm and 77.6 ppm belonging complexes **6** and **7** respectively. The calibration curve based on NMR spectroscopy was constructed by plotting the experimentally observed ratio (NMR) vs. the ratio in which the complexes were mixed. The calibration curve based on mass spectrometry data, was constructed by taken 5 μL aliquots of the NMR samples (diluted in 1.5 mL MeCN), and plotting the ratios of the ESI-MS peak at m/z = 787.09 (**6**) and at *m/z* = 796.09 (**7**), vs. the ratio in which the complexes were mixed. The NMR and ESI-MS data and the corresponding calibration curves are shown in Figures S21-S23.

Conversion of $[LFe_3(HFArPz)_3OFe][OTf]_2$ (1) upon reaction with ^{s}PhIO. In the glovebox, to a solution of $[LFe_3(HFArPz)_3OFe][OTf]_2$ (9.5 mg; 5.1 μmol) in CD_2Cl_2 (0.4 mL) was added a solution of ^{s}PhIO (3.2 mg; 9.4 μmol) in CH_2Cl_2 (0.3 mL). Upon addition, the color changed immediately to black and the solution was stirred for 60 min. The contents were transferred to a NMR tube, and a capillary was added containing a solution of cobaltocene (7.33 mM in CD_2Cl_2). The conversion was recorded by comparing the combined integrals at 47.4, 36.0, 31.8 and 28.2 ppm to the integrals obtained from an authentic solution of $[LFe_3(HFArPz)_2(OArPz)OFe][OTf]_2$ (9.2 mg; 4.9 μmol) in 0.7 mL CD_2Cl_2, containing the same capillary. The conversion was determined to between 40-50%. Based on the integrals ca. 35% is attributed to $[LFe_3(HFArPz)_2(OArPz)OFe][OTf]_2$ (**4**), whereas the remaining 10% is attributed to the formation of $[LFe_3(HFArPz)_2(OFArPz)OFe][OTf]_2$ (**5**) and of $[LFe_3(HFArPz)_3OFe(F)][OTf]_2$ based on the observed product distributions (Figure S28 and S29).

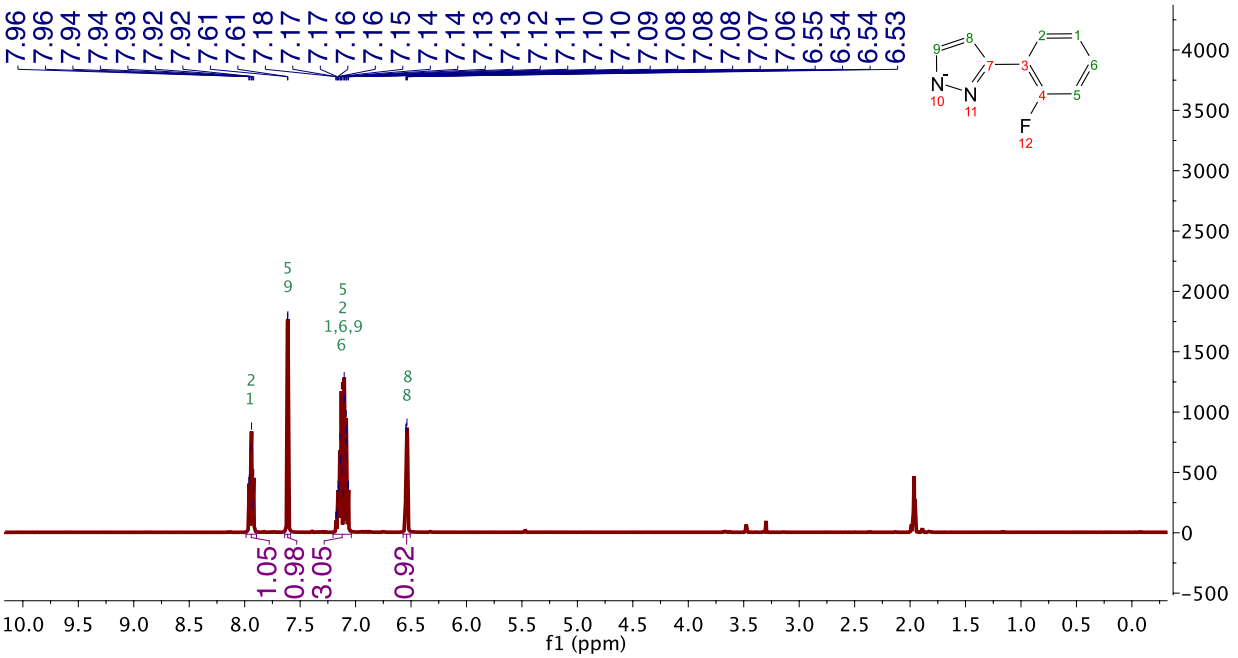

Figure S1. ^{1}H NMR spectrum (400 MHz) of sodium 3-(2-fluorophenyl)pyrazolate (NaHFArPz) in CD_3CN.

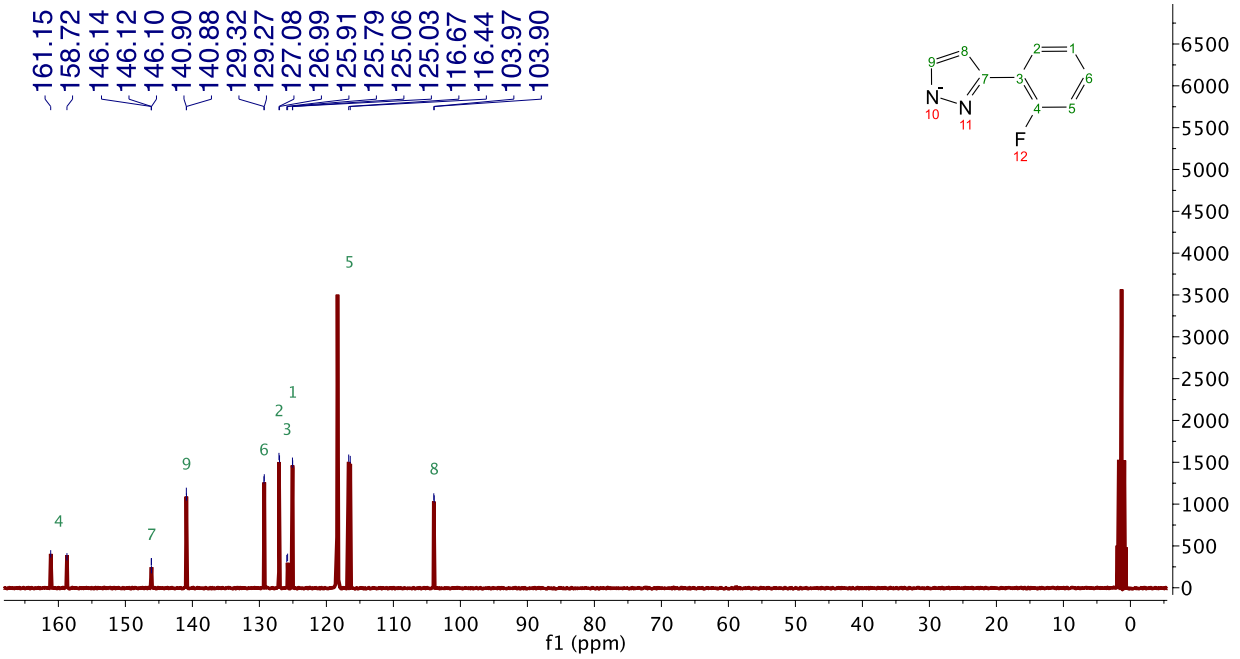

Figure S2. ^{13}C NMR spectrum (101 MHz) of sodium 3-(2-fluorophenyl)pyrazolate (NaHFArPz) in CD_3CN.

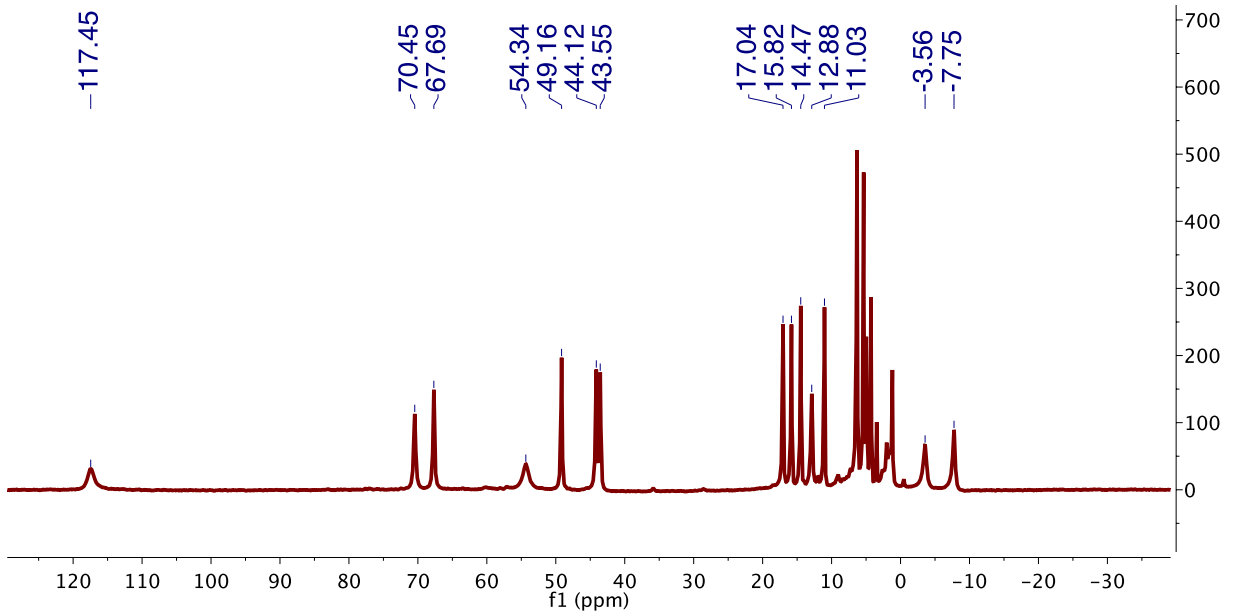

Figure S3. ^{1}H NMR spectrum (300 MHz) of $[LFe_3(HFArPz)_3OFe][OTf]_2$ (**1**) in CD_2Cl_2.

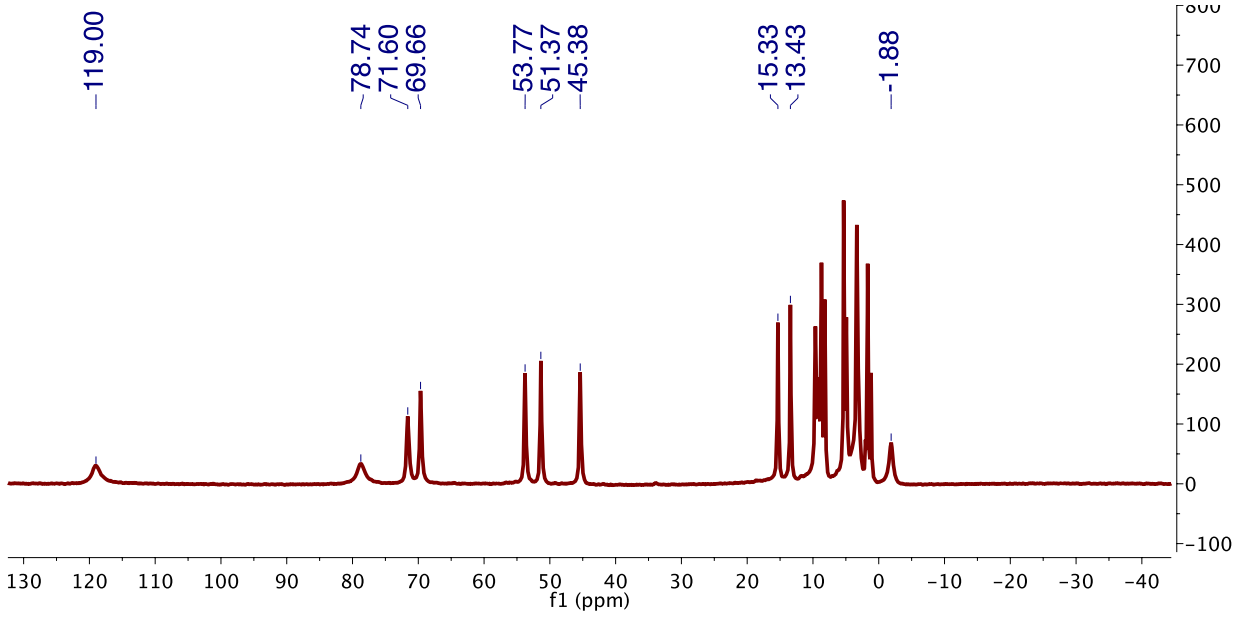

Figure S4. ^{1}H NMR spectrum (300 MHz) of $[LFe_3(HFArPz)_3OMn][OTf]_2$ (**2**) in CD_2Cl_2.

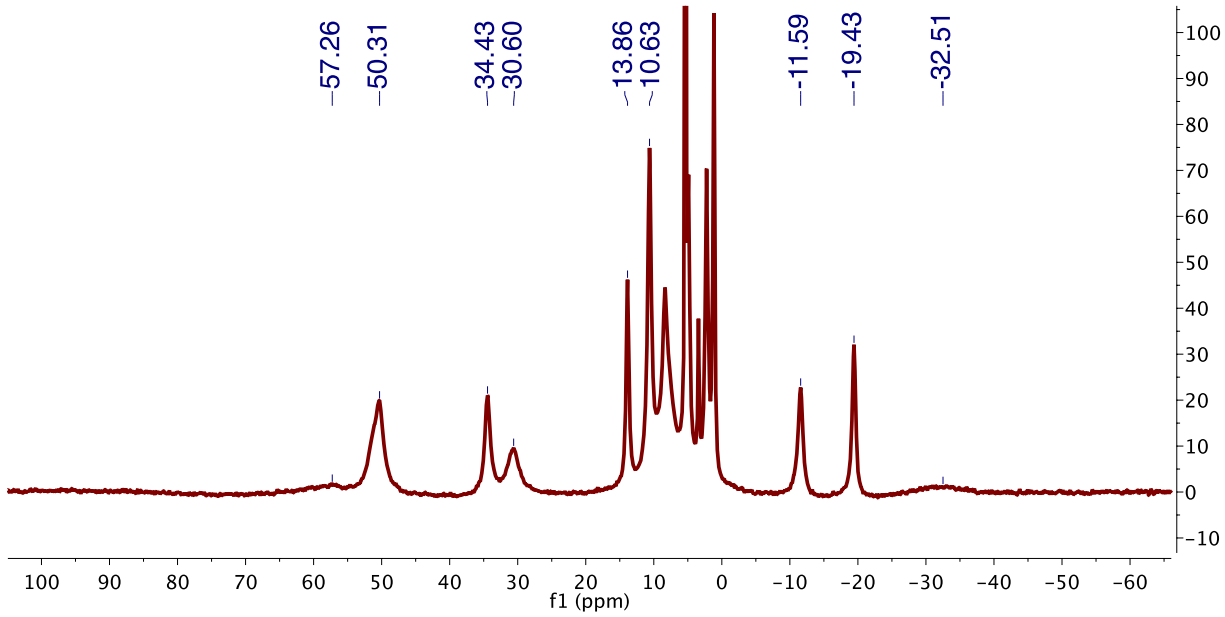

Figure S5. ^{1}H NMR spectrum (300 MHz) of $[LMn_3(HFArPz)_3OMn][OTf]_2$ (**3**) in CD_2Cl_2.

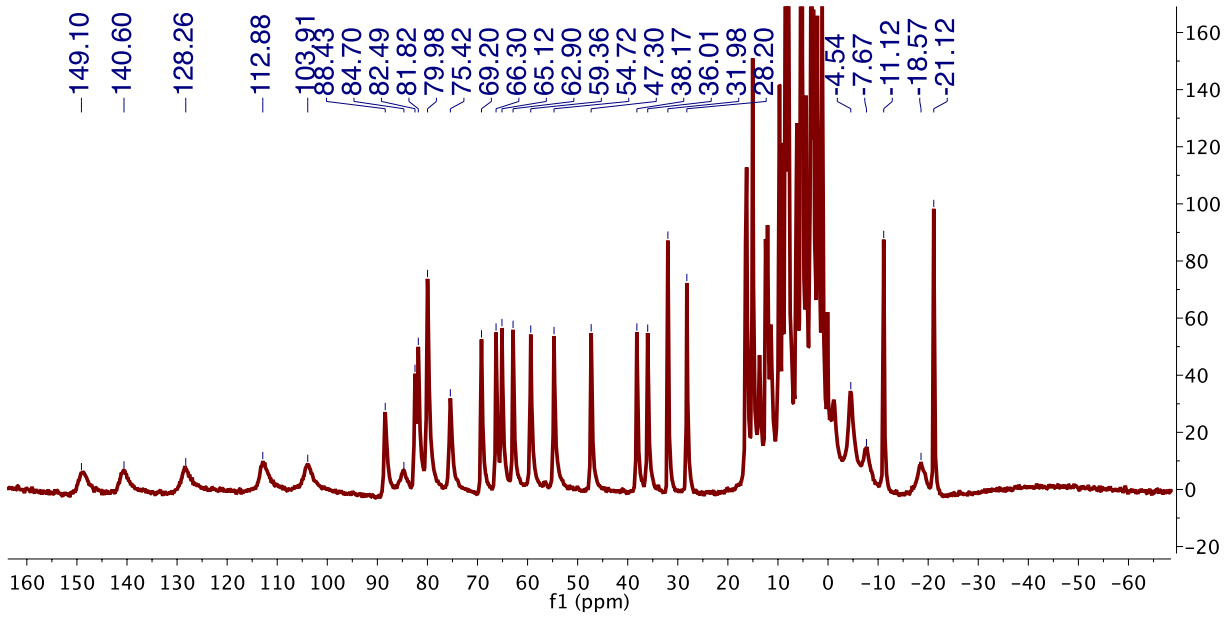

Figure S6. ^{1}H NMR spectrum (300 MHz) of $[LFe_3(HFArPz)_2(OArPz)OFe][OTf]_2$ (**4**) in CD_2Cl_2.

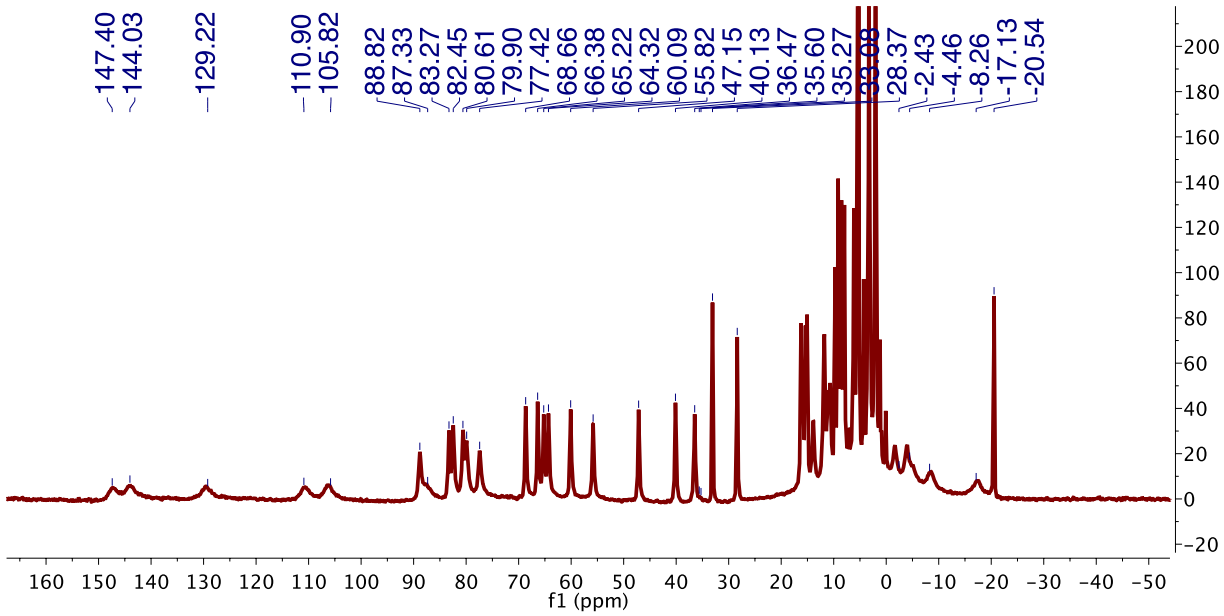

Figure S7. ^{1}H NMR spectrum (300 MHz) of $[LFe_3(HFArPz)_2(OFArPz)OFe][OTf]_2$ (**5**) in CD_2Cl_2.

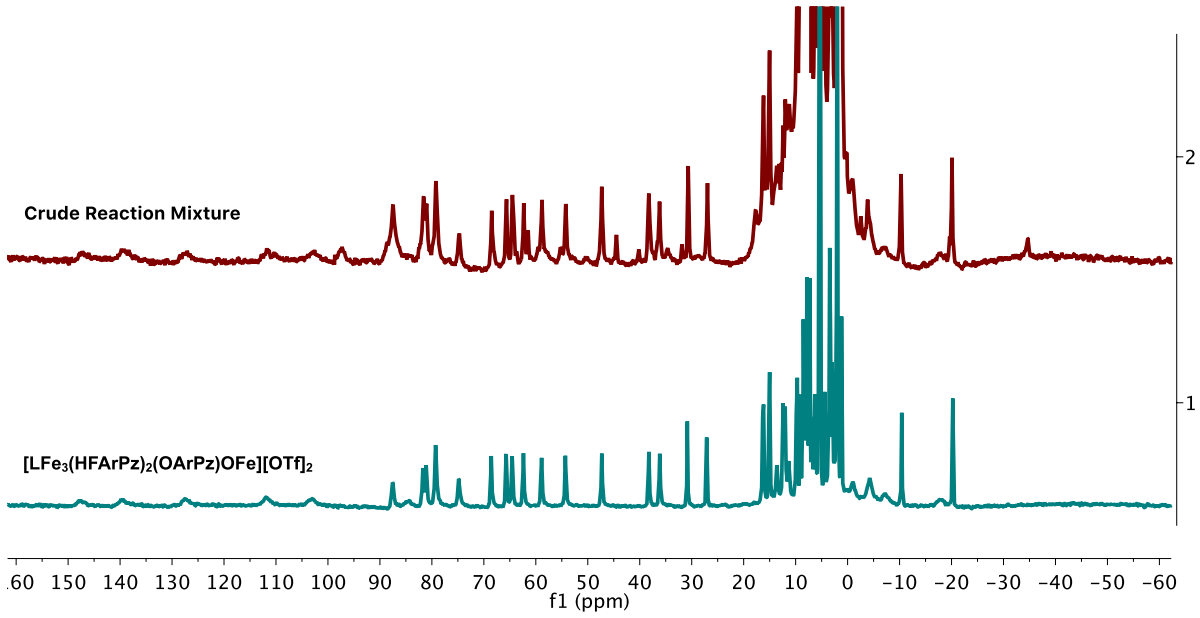

Figure S8. Comparison of the ^{1}H NMR spectrum of the crude reaction mixture with the ^{1}H NMR spectrum of $[LFe_3(HFArPz)_2(OArPz)OFe][OTf]_2$ (**5**) in CD_2Cl_2.

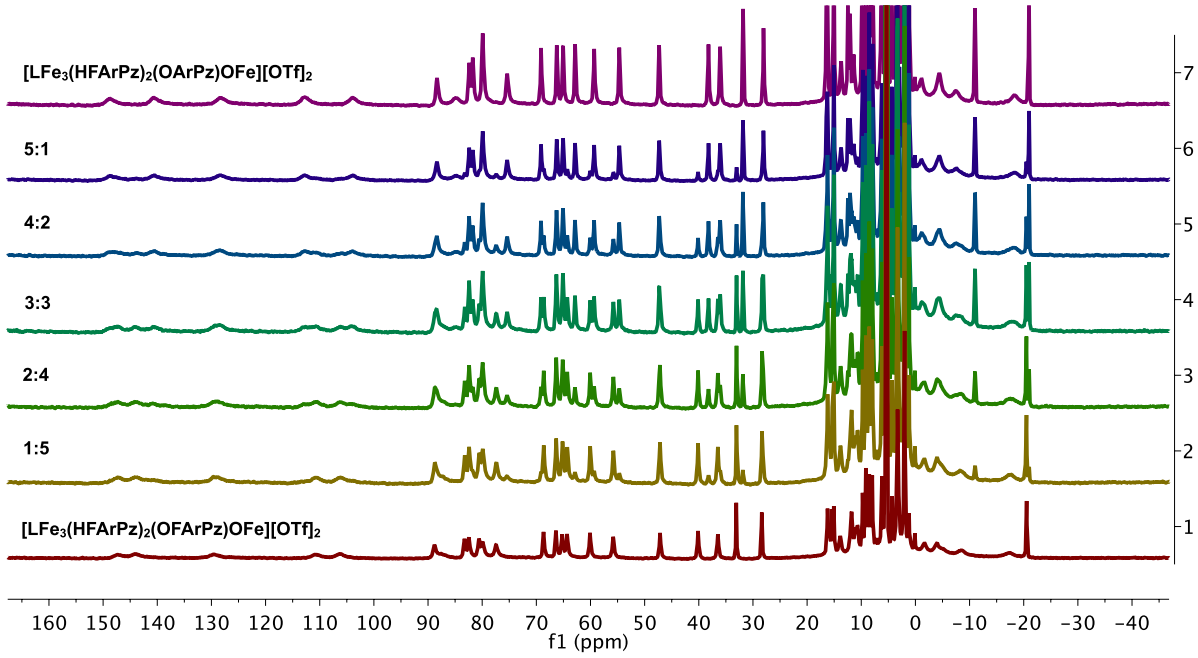

Figure S9. ^{1}H NMR spectrum (300 MHz) of $[LFe_3(HFArPz)_2(OArPz)OFe][OTf]_2$ (**4;** 4.76 mM) and $[LFe_3(HFArPz)_2(OFArPz)OFe][OTf]_2$ (**5**; 4.76 mM) mixed in known ratios to a volume of 0.6 mL in CD_2Cl_2.

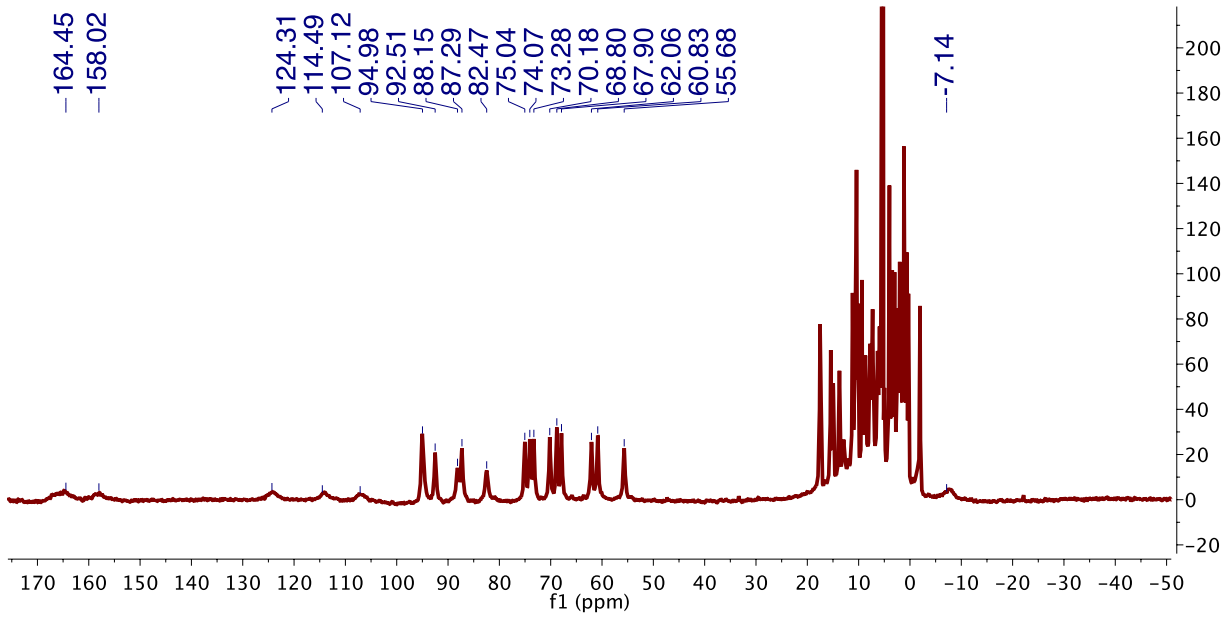

Figure S10. ^{1}H NMR spectrum (300 MHz) of $[LFe_3(HFArPz)_2(OArPz)OMn][OTf]_2$ (**6**) in CD_2Cl_2.

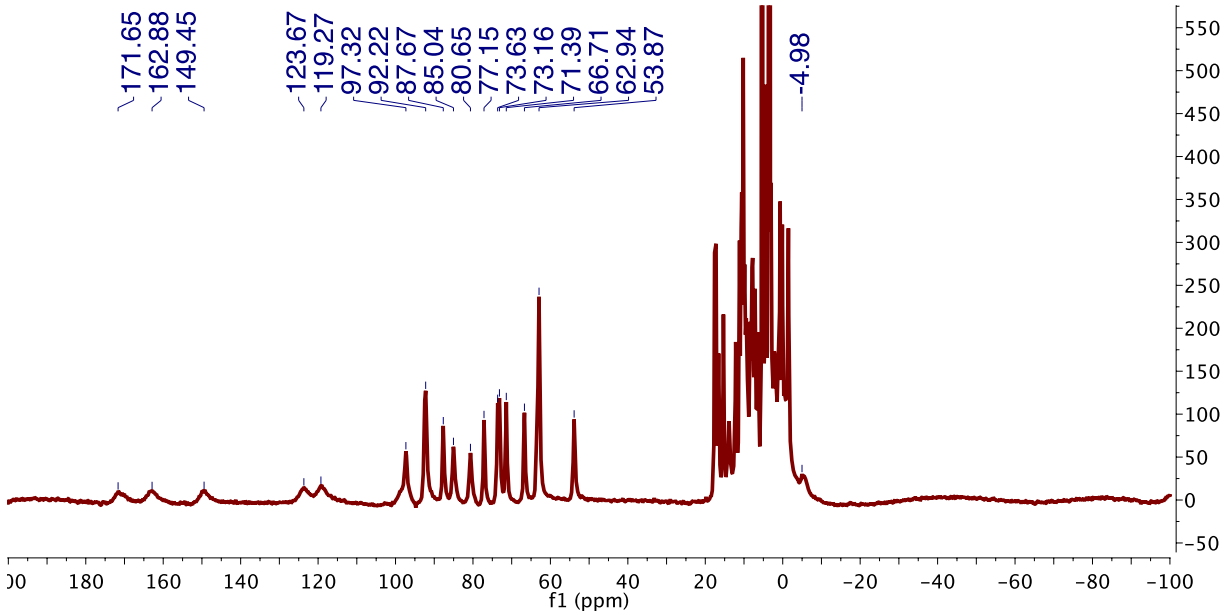

Figure S11. ^{1}H NMR spectrum (300 MHz) of $[LFe_3(HFArPz)_2(OFArPz)OMn][OTf]_2$ (**7**) in CD_2Cl_2.

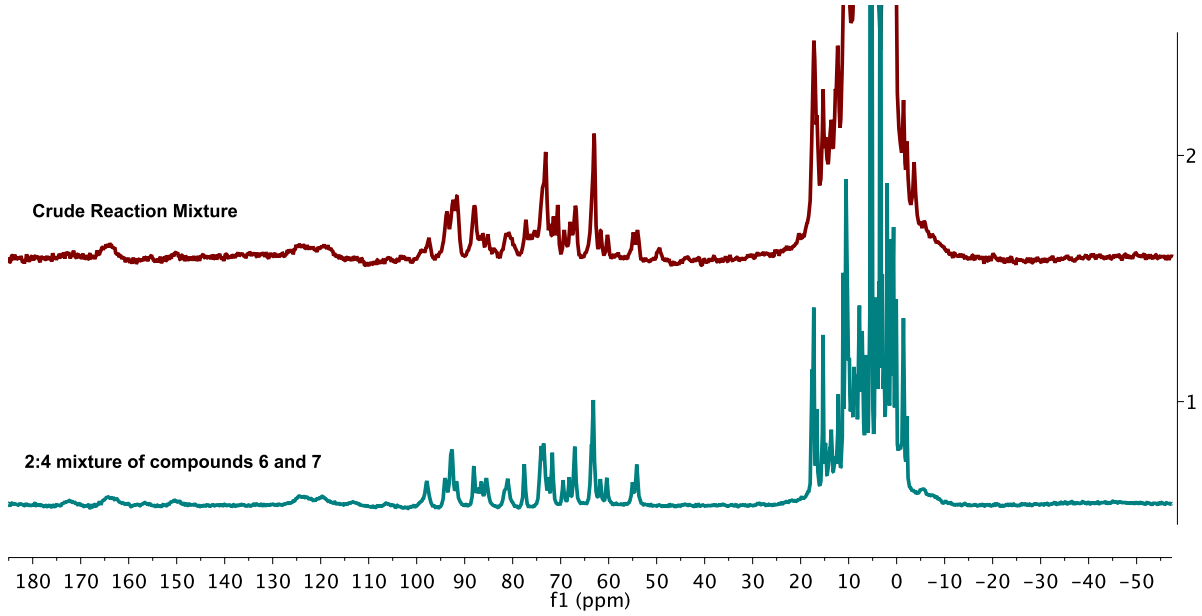

Figure S12. Comparison of the ^{1}H NMR spectrum of the crude reaction mixture with the ^{1}H NMR spectrum of a mixture of $[LFe_3(HFArPz)_2(OArPz)OMn][OTf]_2$ (**6**) and $[LFe_3(HFArPz)_2(OFArPz)OMn][OTf]_2$ (**7**) a 2:4 ratio in CD_2Cl_2.

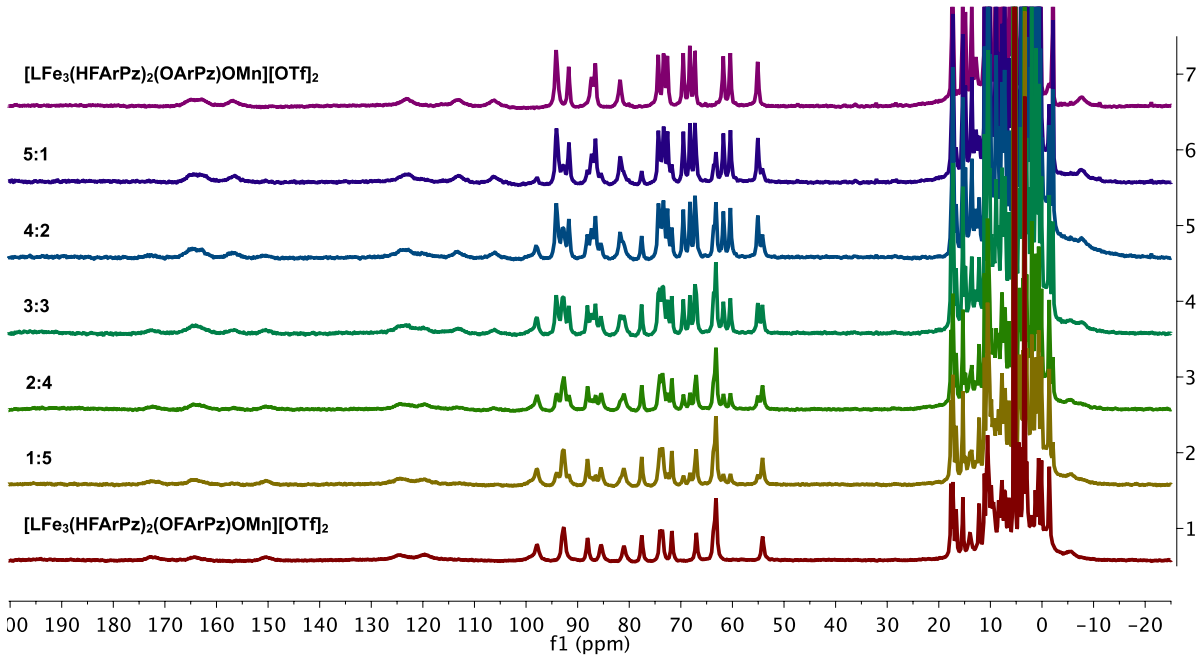

Figure S13. ^{1}H NMR spectrum (300 MHz) of $[LFe_3(HFArPz)_2(OArPz)OMn][OTf]_2$ (**6;** 6.79 mM) and $[LFe_3(HFArPz)_2(OFArPz)OMn][OTf]_2$ (**7**; 6.85 mM) mixed in known ratios to a volume of 0.6 mL in CD_2Cl_2.

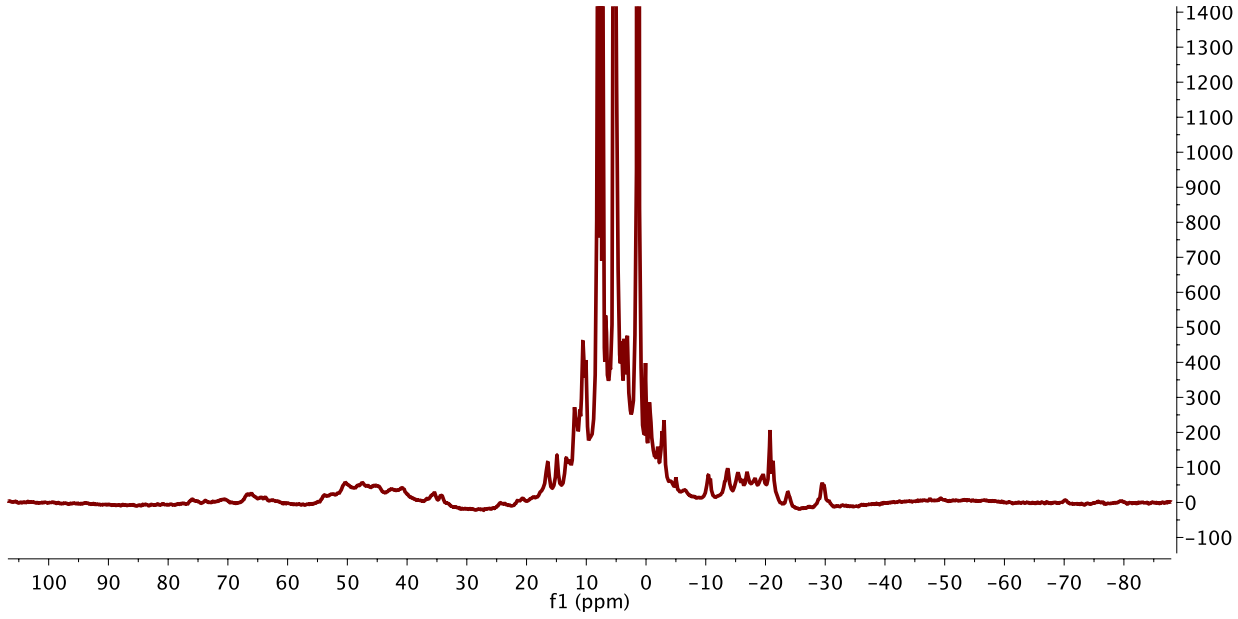

Figure S14. ^{1}H NMR spectrum (300 MHz) of the crude reaction mixture upon treating **3** with ^{s}PhIO for 60 minutes.

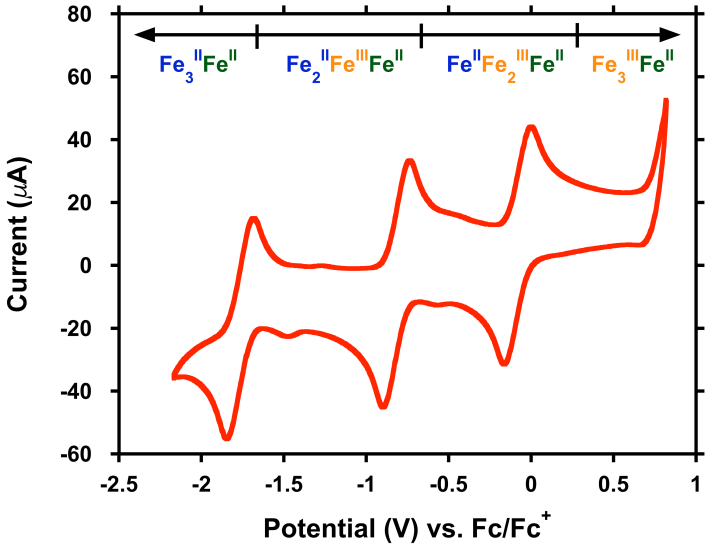

Figure S15. Cyclic voltammogram (CV) of $[LFe_3(HFArPz)_3OFe][OTf]_2$ (**1**) at a scan rate of 100 mV s^{-1}. The CV was recorded in CH_2Cl_2 at a concentration of 2 mM, with glassy carbon, Pt-wire, and Ag-wire as the working, counter, and reference electrodes, respectively. $^nBu_4NPF_6$ (0.1 M) was used as the supporting electrolyte.

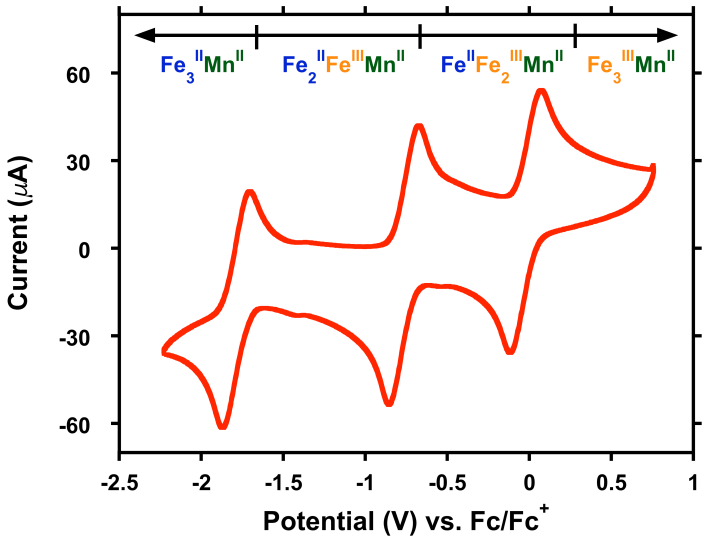

Figure S16. Cyclic voltammogram (CV) of $[LFe_3(HFArPz)_3OMn][OTf]_2$ (**2**) at a scan rate of 100 mV s^{-1}. The CV was recorded in CH_2Cl_2 at a concentration of 2 mM, with glassy carbon, Pt-wire, and Ag-wire as the working, counter, and reference electrodes, respectively. $^nBu_4NPF_6$ (0.1 M) was used as the supporting electrolyte.

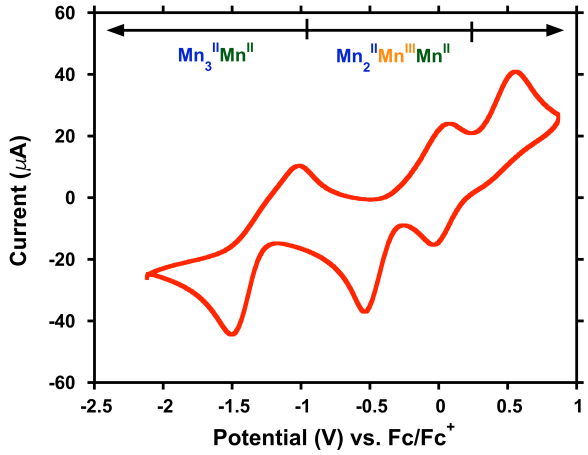

Figure S17. Cyclic voltammogram (CV) of $[LMn_3(HFArPz)_3OMn][OTf]_2$ (**3**) at a scan rate of 100 mV s^{-1}. The CV was recorded in CH_2Cl_2 at a concentration of 2 mM, with glassy carbon, Pt-wire, and Ag-wire as the working, counter, and reference electrodes, respectively. $^nBu_4NPF_6$ (0.1 M) was used as the supporting electrolyte.

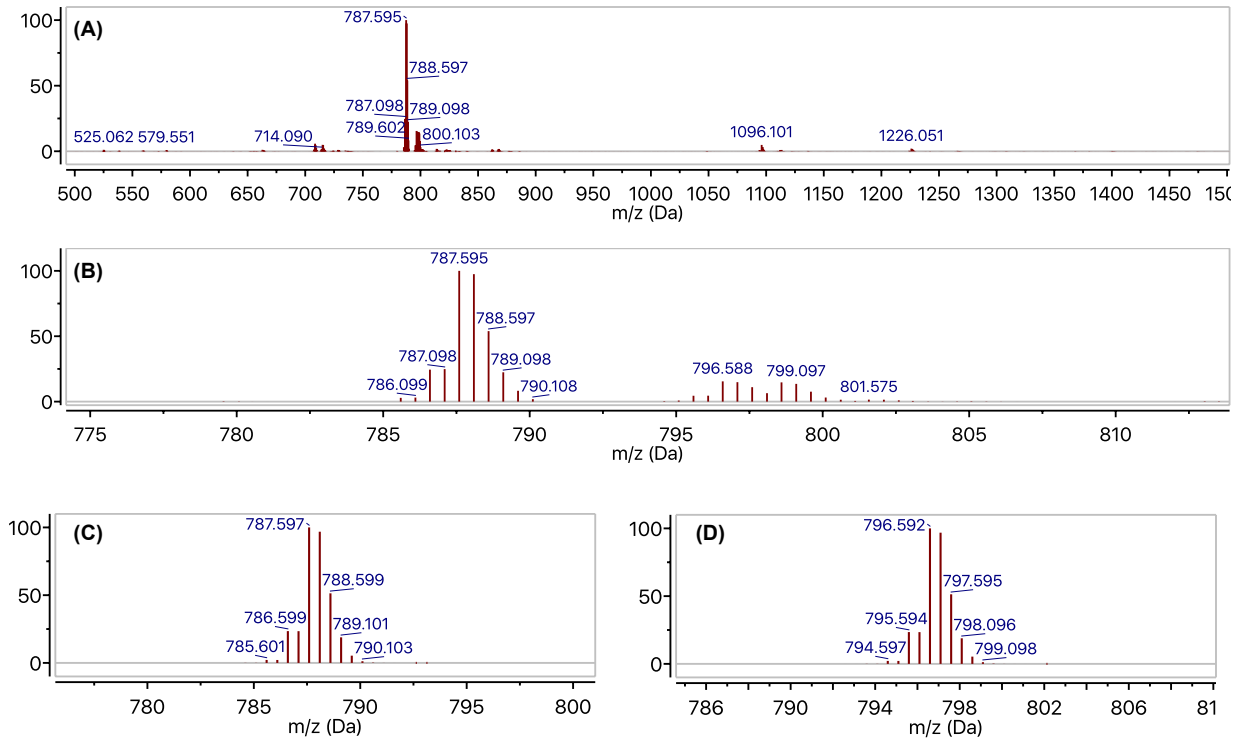

Figure S18. (A and B) Electrospray ionization mass spectrum (ESI-MS) of an aliquot of the crude reaction mixture after treating **1** with ^{s}PhIO (2 equiv.) for 30 minutes in CH_2Cl_2. (C) Simulated mass spectrum and isotope distribution pattern for **4** $[C_{84}H_{57}F_2Fe_4N_{12}O_5]^{2+}$. (D) Simulated mass spectrum and isotope distribution pattern for and **5** $[C_{84}H_{56}F_3Fe_4N_{12}O_5]^{2+}$.

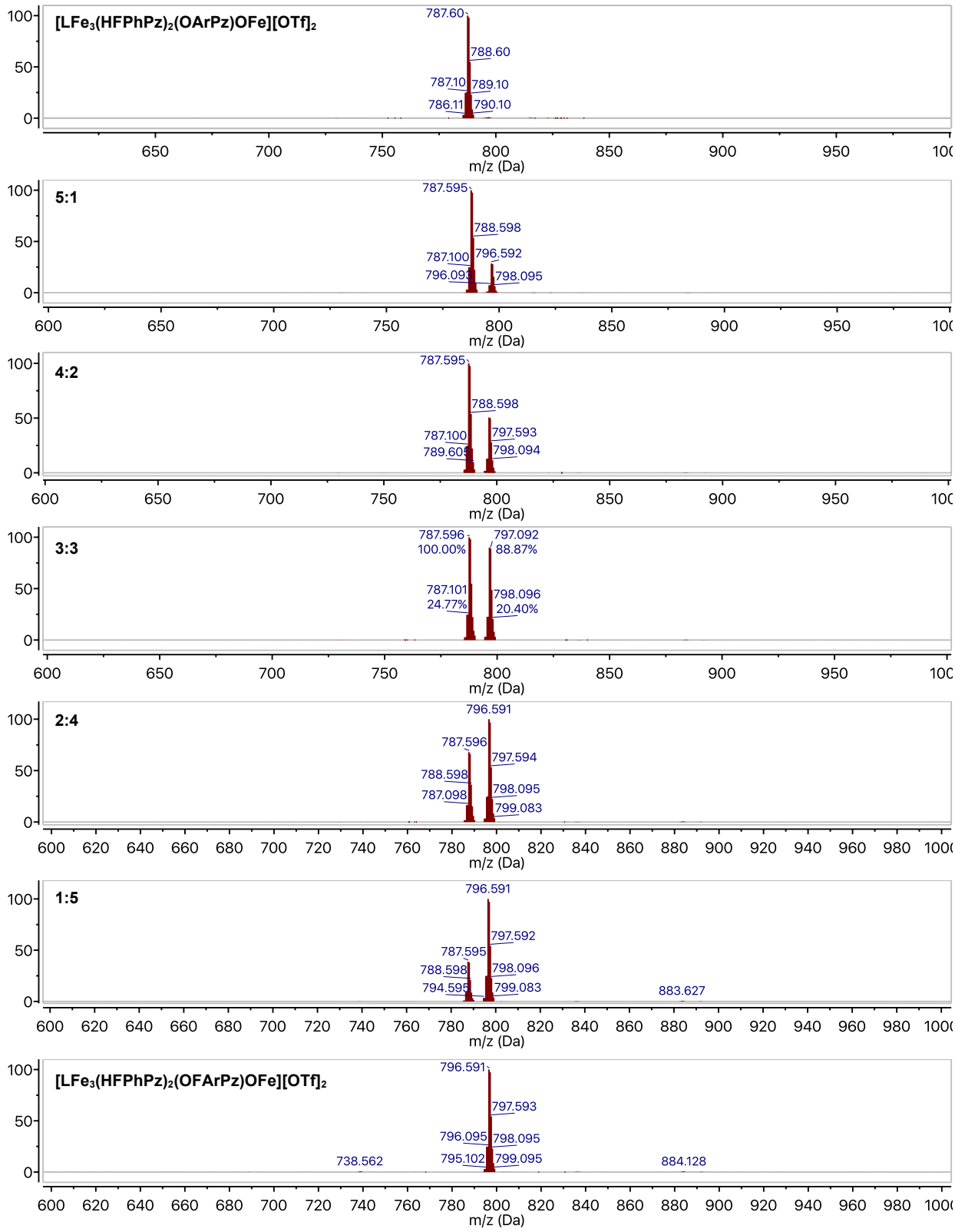

Figure S19. ESI-MS spectra of $[LFe_3(HFArPz)_2(OArPz)OFe][OTf]_2$ (**4;** 4.76 mM, m/z = 787.59) and $[LFe_3(HFArPz)_2(OFArPz)OFe][OTf]_2$ (**5**; 4.76 mM; *m/z* = 796.59) mixed in known ratios in MeCN.

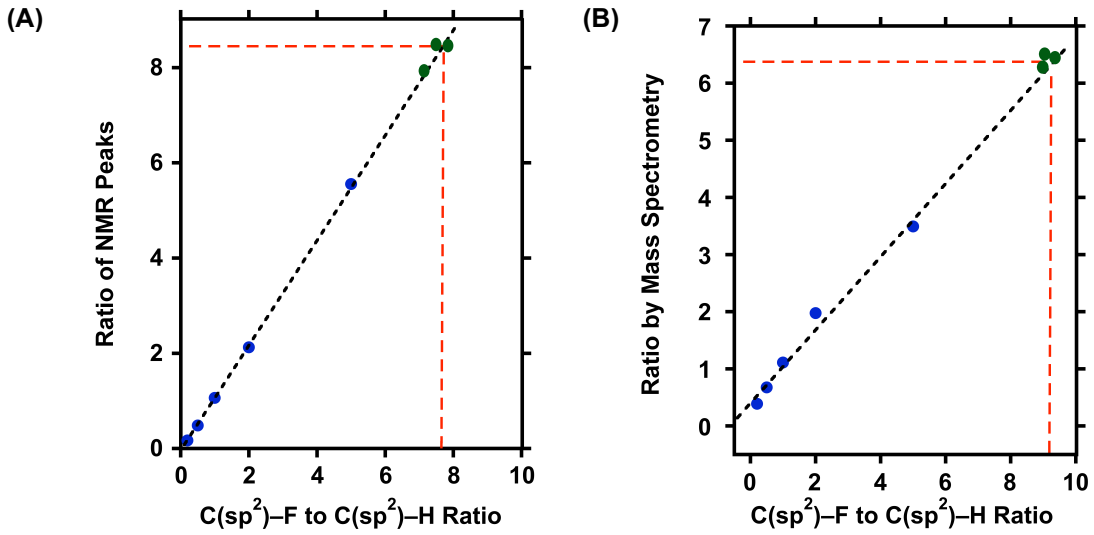

Figure S20. Experimentally determined $C(sp^2)$–F to $C(sp^2)$–H ratio (green dots) by mass spectrometry (A) and ^1H NMR spectroscopy (B). Data points were obtained by either determining the ratio of the relative intensities of the MS peaks at *m/z* = 787.59 (**4**) and at *m/z* = 796.59 (**5**), or by integrating the ^1H NMR resonances at 31.8 ppm and 33.0 ppm belonging to complexes **4** and **5** respectively. The blue dots and dashed black trace (R^2 = 0.99) represent the calibration curve obtained by recording the ratios of the ^1H NMR signals or MS intensities after mixing known concentrations of complexes **4** and **5**.

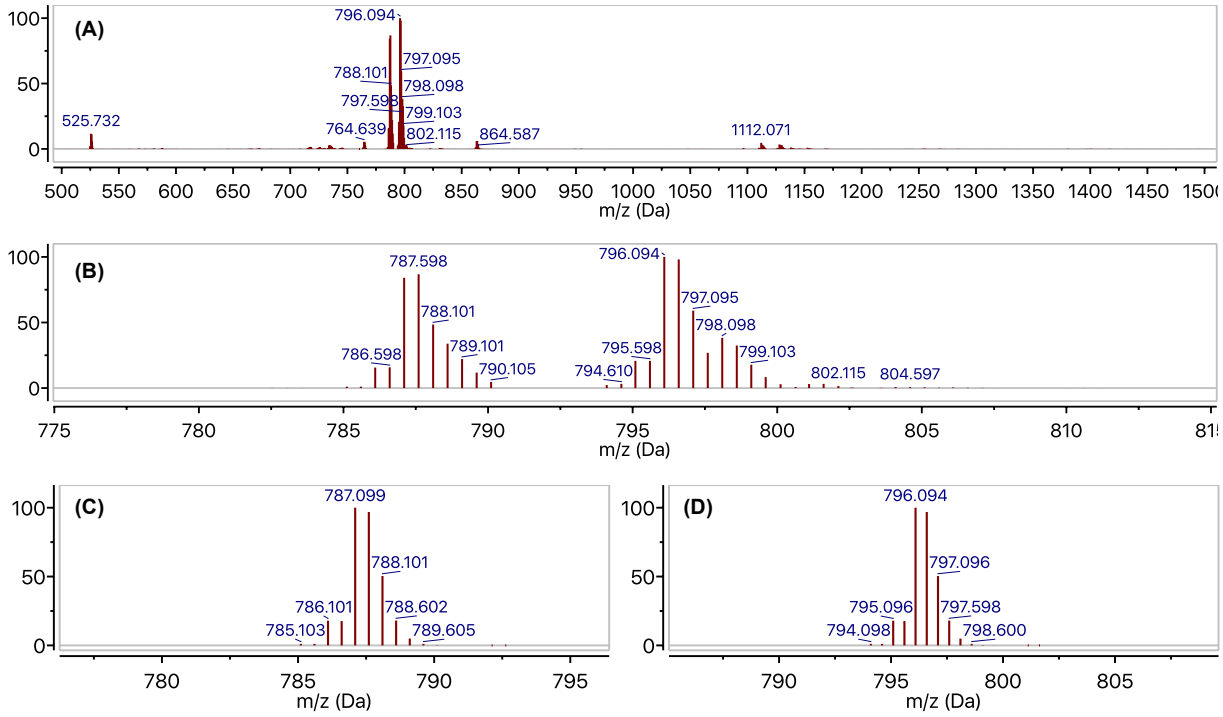

Figure S21. (A and B) Electrospray ionization mass spectrum (ESI-MS) of an aliquot of the crude reaction mixture after treating **2** with ^{s}PhIO (2 equiv.) for 45 minutes in CH_2Cl_2. (C) Simulated mass spectrum and isotope distribution pattern for **6** $[C_{84}H_{57}F_2Fe_3MnN_{12}O_5]^{2+}$. (D) Simulated mass spectrum and isotope distribution pattern for and **7** $[C_{84}H_{56}F_3Fe_3MnN_{12}O_5]^{2+}$. Note: from the isotope distribution pattern, it is evident that there is a small impurity present at *m/z* = 788.59, which is the starting material **2**. However, complex **2** was not observed in the ^{1}H NMR spectrum of the crude reaction mixture.

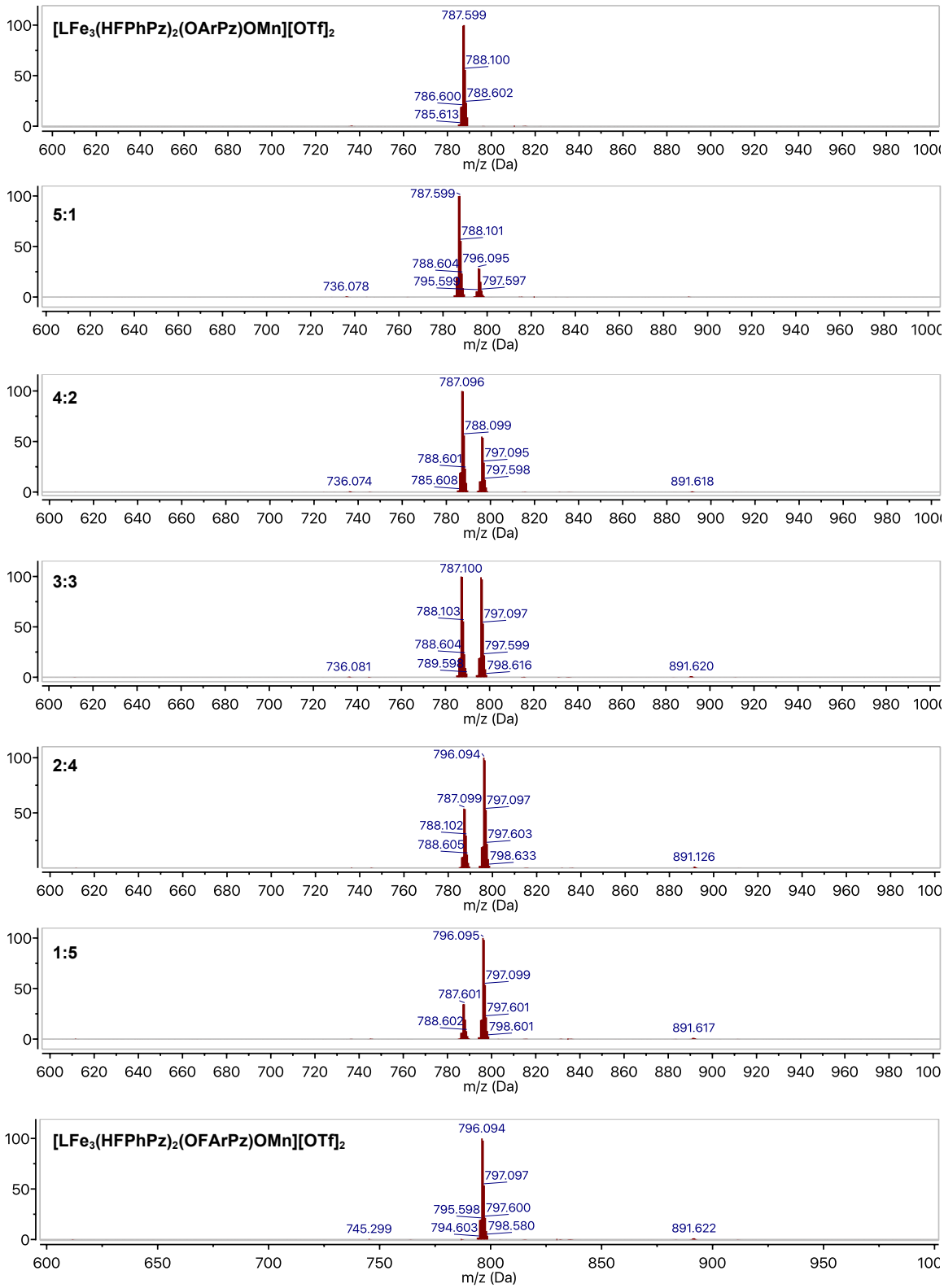

Figure S22. ESI-MS spectra of $[LFe_3(HFArPz)_2(OArPz)OFe][OTf]_2$ (**6;** 6.79 mM, m/z = 787.09) and $[LFe_3(HFArPz)_2(OFArPz)OFe][OTf]_2$ (**7**; 6.85 mM; *m/z* = 796.09) mixed in known ratios in MeCN.

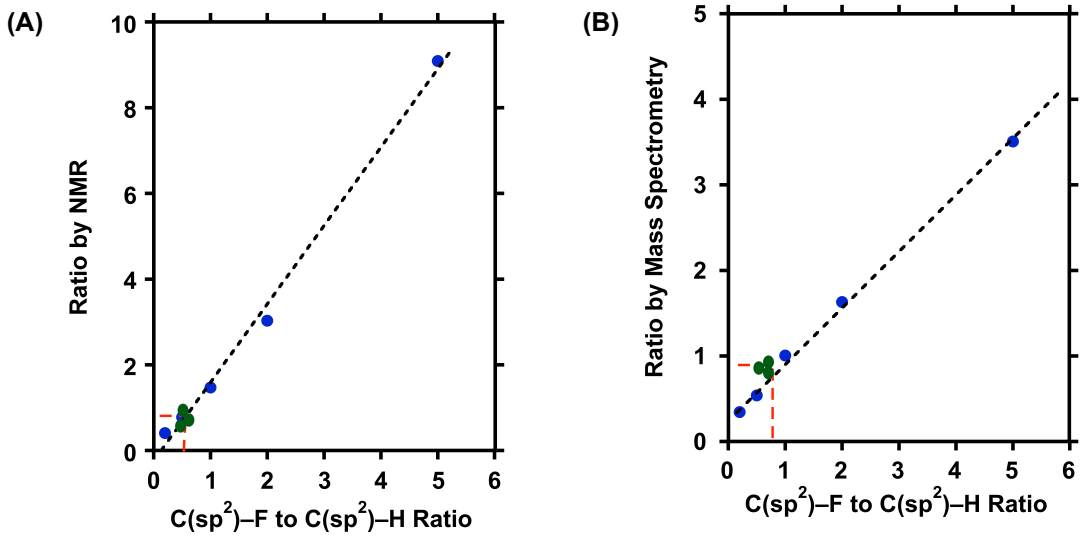

Figure S23. Experimentally determined $C(sp^2)$–F to $C(sp^2)$–H ratio (green dots) by mass spectrometry (A) and ^1H NMR spectroscopy (B). Data points were obtained by either determining the ratio of the relative intensities of the MS peaks at *m/z* = 787.09 (**6**) and at *m/z* = 796.09 (**7**) , or by integrating the ^1H NMR resonances at 60.3 ppm and 77.6 ppm belonging to complexes **6** and **7** respectively. The blue dots and dashed black trace (R^2 = 0.99) represent the calibration curve obtained by recording the ratios of the ^1H NMR signals or MS intensities after mixing known concentrations of complexes **6** and **7**.

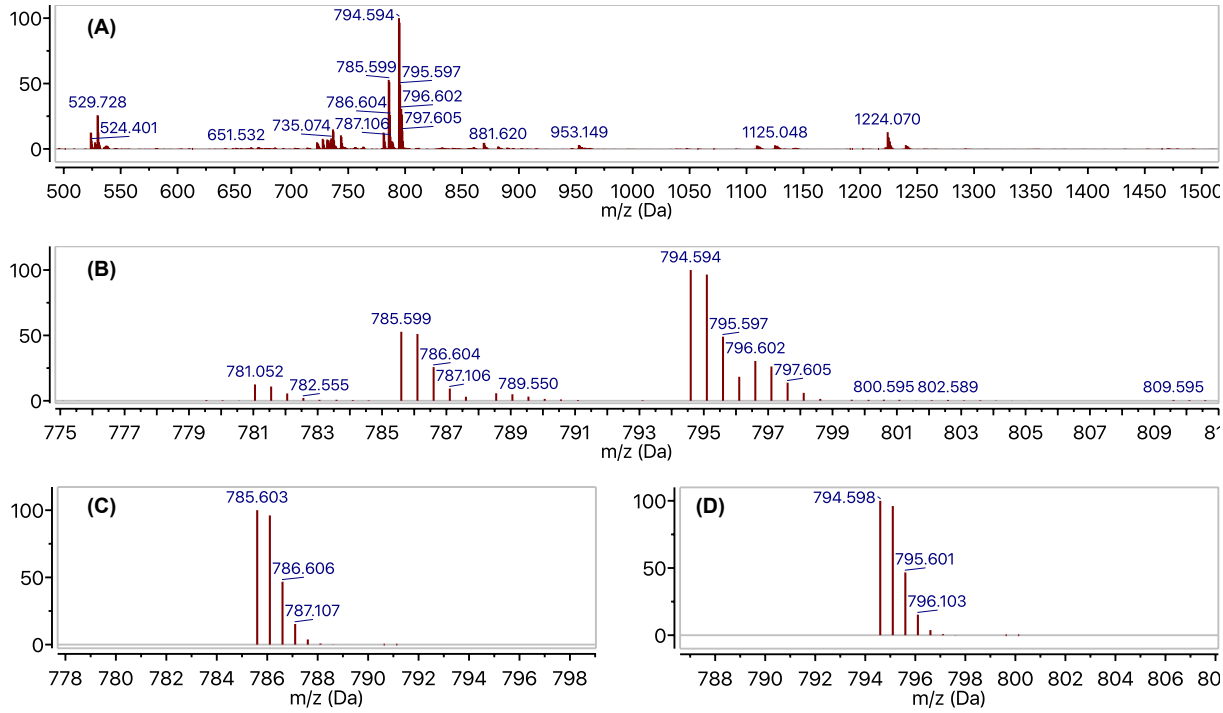

Figure S24. (A and B) Electrospray ionization mass spectrum (ESI-MS) of an aliquot of the crude reaction mixture after treating **3** with ^{s}PhIO (2 equiv.) for 60 minutes in CH_2Cl_2. (C) Simulated mass spectrum and isotope distribution pattern for **8** $[C_{84}H_{57}F_2Mn_4N_{12}O_5]^{2+}$. (D) Simulated mass spectrum and isotope distribution pattern for and **9** $[C_{84}H_{56}F_3Mn_4N_{12}O_5]^{2+}$.

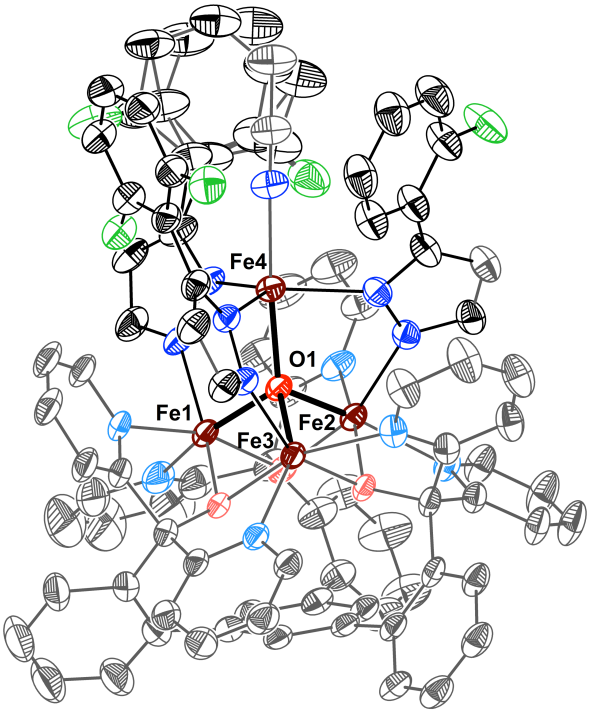

Figure S25. Crystal structure of $[LFe_3(HFArPz)_3OFe][OTf]_2$ (1). Thermal ellipsoids are shown at the 50% probability level. Hydrogen atoms, outer sphere counter ions, and co-crystallized solvents molecules are not shown for clarity.

Special refinement details for complex 1. Compound $[LFe_3(HFArPz)_3OFe][OTf]_2$ (**1**) crystallizes in the monoclinic space group $P2_1/c$ with one molecule in the asymmetric unit along with two triflate anion, 0.4 molecules of diethyl ether, and 1.2 molecules of acetonitrile. Two of the pyrazolate phenyl rings are disordered by rotation, where one is also disordered by vibration, giving rise to *ortho* disordered fluorine substituents. Both disordered fluorine's were modeled as two-component disorder and refined freely to occupancies of 0.63 and 0.37 (ring 1) and 0.59 and 0.41 for the fluorine substituent and phenyl ring on the second pyrazolate. The first triflate anion was modeled as a two-component disordered and refined freely to occupancies of 0.80 and 0.20 respectively. The second triflate counter ion was modelled as a three-component disorder with occupancies of 0.33, 0.36 and 0.31. All disordered triflates were refined with the help of similarity restraints on the 1,2- and 1,3-distances and displacement parameters. One acetonitrile molecule (occupancy 0.7) is disordered is disordered over three positions and refined with occupancies of 0.22, 0.22 and 0.26. This heavily discorded acetonitrile molecule did not refine anisotropically and all atoms were modelled with ISOR restraints, and with distance restraints on the 1,2- and 1,3-distances. All the triflate counter ions, acetonitrile molecules, and diethyl ether molecules were refined with the help of enhanced rigid bond restraints for anisotropic displacement parameters. In addition, all atoms were refined with rigid bond restraints, and restrained to have similar U_{ij} values.

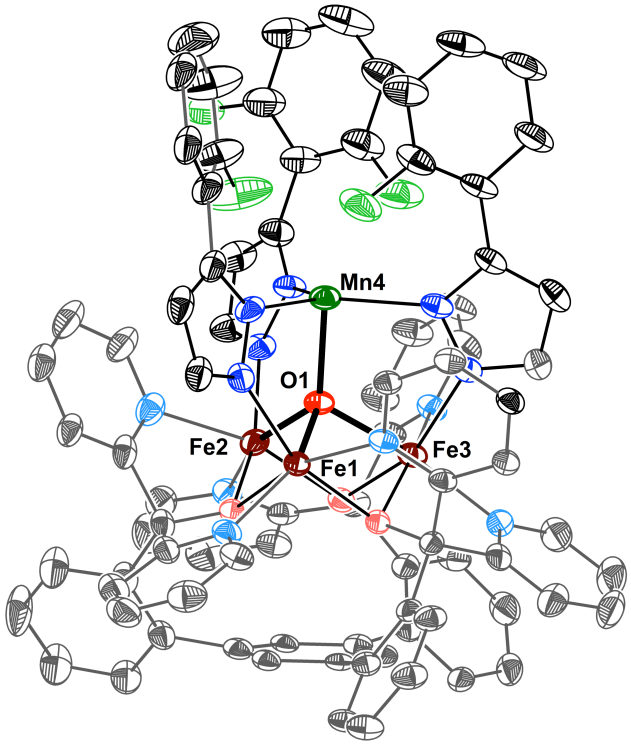

Figure S26. Crystal structure of $[LFe_3(HFArPz)_3OMn][OTf]_2$ (2). Thermal ellipsoids are shown at the 50% probability level. Hydrogen atoms, outer sphere counter ions, and co-crystallized solvents molecules are not shown for clarity.

Special refinement details for complex 2. Complex **2** crystallizes in the monoclinic space group *C*2*c* with one molecule in the asymmetric unit along with two triflate anions, 1.34 molecules of diethyl ether and 3.24 molecules of acetonitrile. One the pyrazolate phenyl rings is disordered by rotation, giving rise to *ortho* disordered fluorine substituents. Both disordered fluorine atoms were modeled as a two-component disorder and refined freely to occupancies of 0.57 and 0.43 respectively. One of the triflate anions was disordered over two positions, and refined freely with occupancies of 0.41 and 0.59. The diethyl ethyl and acetonitrile are located in large solvent accessible voids and highly disordered. The diethyl ether was modeled over five positions and the acetonitrile was modeled over six positions. All disordered atoms were refined with the help of similarity restraints on the 1,2- and 1,3-distances and displacement parameters as well as enhanced rigid bond restraints for anisotropic displacement parameters

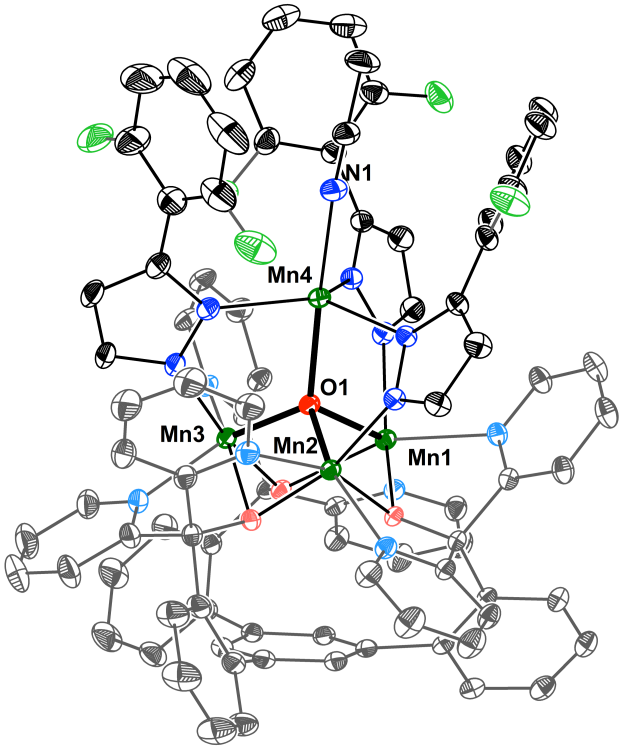

Figure S27. Crystal structure of $[LMn_3(HFArPz)_3OMn][OTf]_2$ (3). Thermal ellipsoids are shown at the 50% probability level. Hydrogen atoms, outer sphere counter ions, and co-crystallized solvents molecules are not shown for clarity.

Special refinement details for complex 3. Compound $[LMn_3(HFArPz)_3OFe][OTf]_2$ (**3**) crystallizes in the monoclinic space group $P2_1/c$ with one molecule in the asymmetric unit along with two triflate anion, 1.2 molecules of diethyl ether, and 2.3 molecules of acetonitrile. Two of the pyrazolate phenyl rings are discorded by rotation, giving rise to *ortho* disordered fluorine substituent. Both disordered fluorine's were modeled as two-component disorder and refined freely to occupancies of 0.66 and 0.33 (ring 1) and 0.73 and 0.27 for the fluorine substituent on the second pyrazolate phenyl ring. One of triflate anions is disordered and was modelled as a three-component disorder with fixed occupancies of 0.10, 0.30 and 0.60 respectively. The disordered triflate was refined with the help of similarity restraints on the 1,2- and 1,3-distances and displacement parameters. One diethyl ether molecule is disordered with two acetonitrile molecules and was modelled as a three-component disorder with occupancies of 0.20 for the diethyl ether molecule and 0.40 for both acetonitrile molecules. The co-crystallized diethyl ether molecules were refined, while restraining the 1,2- and 1,3-distances. All triflate counter ions and solvent molecules were refined with the help of enhanced rigid bond restraints for anisotropic displacement parameters.

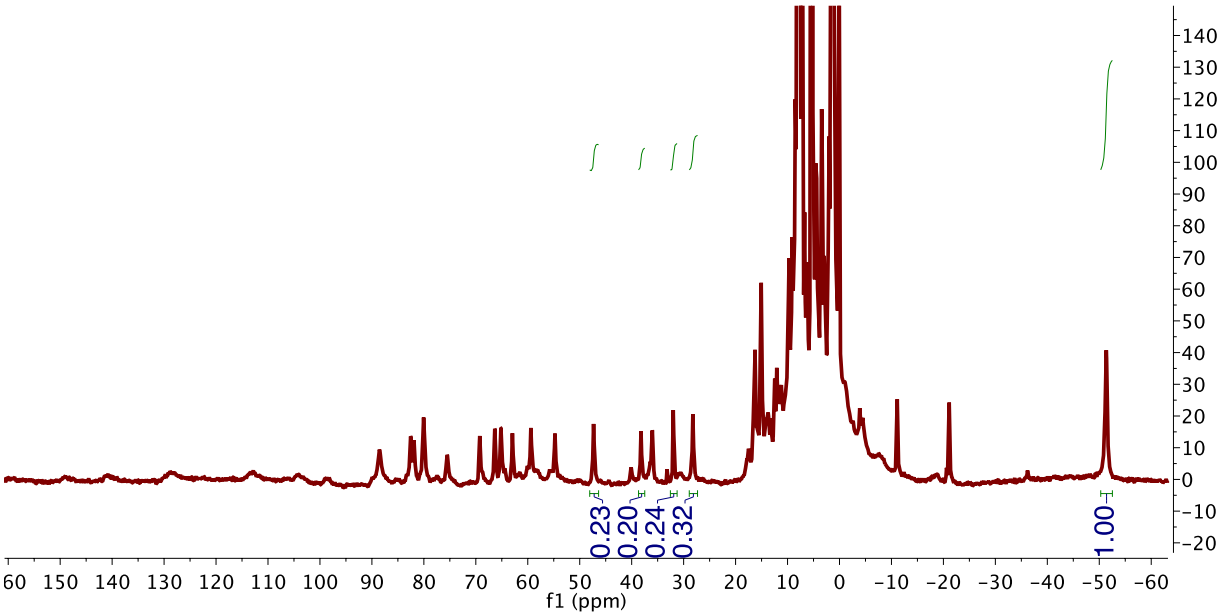

Figure S28. ^{1}H NMR spectrum (300 MHz) of the crude reaction mixture upon treating **1** with ^{s}PhIO for 45 minutes, in the presence of an internal standard ($CoCp_2$; 7.33mM) in a glass capillary.

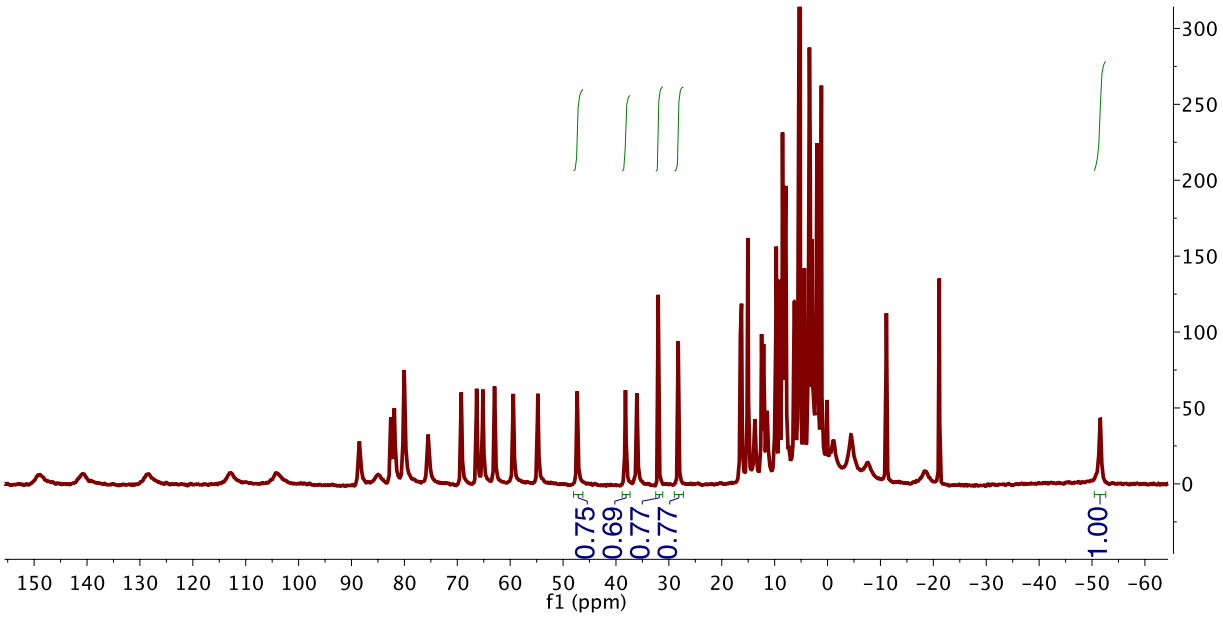

Figure S29. ^{1}H NMR spectrum (300 MHz) of **4** in the presence of an internal standard ($CoCp_2$; 71.4 mM) in a glass capillary.

Table S1. Selected bond angles and distances for complexes **1**–**3**.

Bond Distance (Å)	**Complex**		
	1	**2** [a]	**3**
M1–O1	1.915(3)	1.978(4)	2.2244(13)
M2–O1	1.938(3)	1.958(4)	1.8977(12)
M3–O1	2.144(3)	2.107(4)	1.8914(13)
M1–N13	2.090(3)	2.101(5)	2.3136(16)
M2–N23	2.072(4)	2.149(5)	2.0128(16)
M3–N33	2.113(3)	2.117(5)	2.0050(16)
M4–N14	2.127(4)	2.172(6)	2.1390(16)
M4–N24	2.131(3)	2.172(5)	2.1913(15)
M4–N34	2.090(3)	2.148(5)	2.1888(17)
M4-N1	2.120(4)	-	2.2030(18)
N13–N14	1.374(5)	1.383(7)	1.369(2)
N23–N24	1.378(5)	1.382(6)	1.368(2)
N33–N34	1.378(4)	1.365(7)	1.371(2)
M4–O1	2.048(3)	1.996(4)	2.0901(13)
Bond Angles (°)			
N14–Mn4–N24	125.74(14)	121.2(2)	110.74(6)
N24–Mn4–N34	114.38(13)	117.9(2)	127.31(6)
N34–Mn4–N14	118.13(14)	120.71(19)	118.94(6)
O1–Mn4–N1	175.06(14)	-	171.62(6)

Table S2. Crystal and refinement data for complexes **1**–**3**.

	Complex **1**	Complex **2**	Complex **3**
CCDC			
Empirical formula	$C_{92}H_{67.6}F_9Fe_4N_{14.2}O_{10.4}S_2$	$C_{97.88}H_{80.13}N_{15.23}O_{11.34}F_9S_2Fe_3Mn$	$C_{97.4}H_{78.9}F_9Mn_4N_{15.3}O_{11.2}S_2$
Formula weight (g/mol)	1996.92	2108.82	2097.73
T (K)	100	100	100
Radiation	MoKα (λ = 0.71073)	CuKα (λ = 1.54178)	MoKα (λ = 0.71073)
a (Å)	22.7641(10)	24.5890(14)	22.9197(16)
b (Å)	17.3323(8)	30.9989(16)	17.2938(12)
c (Å)	24.0740(11)	24.9769(12)	24.1821(17)
α (deg)	90	90	90
β (deg)	97.1460(10)	95.136(3)	96.961(4)
γ (deg)	90	90	90
V (Å^3)	9424.7(7)	18961.8(17)	9514.4(12)
Z	4	8	4
Cryst. syst.	monoclinic	monoclinic	monoclinic
Space group	$P2_1/c$	$C2/c$	$P2_1/c$
$\rho_{calc}g$ (cm^3)	1.407	1.477	1.464
2 σ range (deg)	4.7 to 57.398	4.598 to 148.99	2.902 to 72.944
Crystal size/mm	0.33 × 0.24 × 0.17	0.25 × 0.22 × 0.11	0.20 × 0.20 × 0.20
μ (mm^{-1})	0.730	5.820	0.649
GOF	1.068	1.047	1.061
R1, wR2 (I> 2σ (I))	$R_1 = 0.0777$, $wR_2 = 0.2204$	$R_1 = 0.0950$, $wR_2 = 0.2287$	$R_1 = 0.0614$, $wR_2 = 0.1621$

References

[S1] C.-Y. Huang, A. G. Doyle, *J. Am. Chem. Soc.* **2012**, *134*, 9541-9544.

[S2] F. Song, C. Wang, J. M. Falkowski, L. Ma, W. Lin, *J. Am. Chem. Soc.* **2010**, *132*, 15390-15398.

[S3] D. Macikenas, E. Skrzypczak-Jankun, J. D. Protasiewicz, *J. Am. Chem. Soc.* **1999**, *121*, 7164-7165.

[S4] G. de Ruiter, N. B. Thompson, D. Lionetti, T. Agapie, *J. Am. Chem. Soc.* **2015**, *137*, 14094-14106.

[S5] C. Liu, K. Leftheris, J. Lin, Preparation of benzothiazole and azabenzothiazole compounds useful as kinase inhibitors, WO2007016392A2, Bristol-Myers Squibb Company, USA . **2007**, 95pp.

[S6] G. de Ruiter, N. B. Thompson, M. K. Takase, T. Agapie, *J. Am. Chem. Soc.* **2016**, *138*, 1486-1489.

[S7] E. Y. Tsui, J. S. Kanady, M. W. Day, T. Agapie, *Chem. Commun.* **2011**, *47*, 4189-4191.

[S8] APEX-II, *Version 2 User Manual, M86-E01078, Bruker Analytical X-ray Systems,*, Madison, WI, **June 2006.**

[S9] G. M. Sheldrick, *"SADABS (version 2008/1): Program for Absorption Correction for Data from Area Detector Frames",* , University of Göttingen, **2008**.

[S10] G. Sheldrick, *Acta Crystallogr., Sect. A* **1990**, *46*, 467-473.

[S11] G. M. Sheldrick, *Acta Crystallogr., Sect. A: Found. Crystallogr.* **2008**, *64*, 112-122.

[S12] P. Müller, *Crystallogr. Rev.* **2009**, *15*, 57-83.